# Robust SINR-Constrained Symbol-Level Multiuser Precoding with Imperfect Channel Knowledge

Alireza Haqiqatnejad, *Student Member, IEEE*, Farbod Kayhan, and Björn Ottersten, *Fellow, IEEE*

***Abstract*—In this paper, we address robust design of symbol-level precoding (SLP) for the downlink of multiuser multiple-input single-output wireless channels, when imperfect channel state information (CSI) is available at the transmitter. In particular, we consider a well known model for the CSI imperfection, namely, stochastic Gaussian-distributed uncertainty. Our design objective is to minimize the total (per-symbol) transmission power subject to constructive interference (CI) constraints as well as the users' quality-of-service requirements in terms of signal-to-interference-plus-noise ratio. Assuming stochastic channel uncertainties, we first define probabilistic CI constraints in order to achieve robustness to statistically known CSI errors. Since these probabilistic constraints are difficult to handle, we resort to their convex approximations in the form of tractable (deterministic) robust constraints. Three convex approximations are obtained based on different conservatism levels, among which one is introduced as a benchmark for comparison. We show that each of our proposed approximations is tighter than the other under specific robustness settings, while both of them always outperform the benchmark. Using the proposed CI constraints, we formulate the robust SLP optimization problem as a second-order cone program. Extensive simulation results are provided to validate our analytic discussions and to make comparisons with conventional block-level robust precoding schemes. We show that the robust design of symbol-level precoder leads to an improved performance in terms of energy efficiency at the cost of increasing the computational complexity by an order of the number of users in the large system limit, compared to its non-robust counterpart.**

***Index Terms*—Downlink MU-MISO, imperfect CSI, symbol-level precoding, stochastic optimization, stochastic robust design.**

## I. Introduction

MULTIUSER precoding is a well known technique to enhance the achievable throughput and the reliability of communication in a downlink multiuser multiple-input single-output (MU-MISO) wireless system. In principle, this improvement is brought by employing multiple antennas at the transmitter, which enables more degrees of freedom to manage the channel-induced multiuser interference (MUI). In most applications, however, the system might be subject to some crucial system-centric and/or user-specific requirements, e.g., transmission power constraint or quality-of-service (QoS) targets. In such scenarios, the precoding design problem needs to be constrained by the given requirements while aiming at optimizing a certain objective function; this type of design is often called objective-oriented precoding optimization [1]. Among a variety of design criteria, a frequently addressed one is the QoS-constrained power minimization; see, e.g., [2]–[4].

In general, multiuser precoding schemes can be categorized in two groups, namely, conventional (block-level) techniques and symbol-level techniques. In the conventional precoding, the precoder typically exploits the channel knowledge in order to suppress/eliminate the MUI, regardless of the current users' symbols [5], [6]. On the contrary, in the symbol-level design, the basic idea is to convert the (potential) MUI into a desired received signal component, i.e., into the so-called constructive interference (CI), by means of processing the transmit signal on a symbol-level basis [7], [8].

In reality, assuming perfect channel state information (CSI), either statistically or instantaneously, is rather impractical due to various inevitable channel impairments such as imperfect channel estimation, limited feedback, or latency-related errors [9]–[11]. However, potential performance improvements may no longer be offered by multiuser precoding if accurate CSI is not available at the transmitter, broadly because precoding techniques are quite sensitive to channel uncertainties [10]. One may expect an even more adverse effect of imperfect channel knowledge on the symbol-level precoder's performance due to the fact that the promised efficiency (extremely) depends on the satisfaction of CI constraints in order to successfully accommodate each (noise-free) received signal in the correct CI region. To alleviate this reliance, the problem of designing a multiuser precoder that is robust to channel uncertainties becomes of practical interest.

The channel uncertainty region is commonly considered to be either ellipsoidal or stochastic, or a combination of both, e.g., see [12]. Under the ellipsoidal uncertainty model, usually no assumption is made on the distribution of the CSI error, but the error is assumed to always lie within a bounded region. This kind of modeling, which ultimately leads to a worst-case analysis, is known to appropriately capture the bounded uncertainties resulted from quantization errors [13]. The stochastic uncertainty model, on the other hand, assume that the statistical properties of the CSI error is known. In scenarios with channel estimation at the transmitter/receiver side, such modeling is particularly suitable since the error in the estimation process can often be treated as a Gaussian random variable [14].

With a particular focus on MU-MISO broadcast channels, a wide variety of robust schemes can be found in the literature on conventional multiuser precoding, addressing both bounded and stochastic uncertainty models. In this line of work, most of the existing research considers either the QoS-constrained power minimization or the max-min fairness with power constraints as the design formulation. Under norm-bounded

The authors are with the Interdisciplinary Centre for Security, Reliability and Trust (SnT), University of Luxembourg, Luxembourg City L-1855, Luxembourg (e-mail: alireza.haqiqatnejad@uni.lu; farbod.kayhan@uni.lu; bjorn.ottersten@uni.lu).

This paper has been presented in part at the IEEE Global Communications Conference (GLOBECOM), Abu Dhabi, UAE, 2018.

CSI uncertainty, the QoS problem is typically constrained by the worst signal-to-interference-plus-noise ratio (SINR) among the users, resulting in highly conservative design approaches; see, e.g., [15]–[17] as some notable research in this direction. These worst-case SINR requirements can also be translated to worst-case minimum mean-square error (MMSE) constraints [18], [19]. Assuming Gaussian-distributed stochastic CSI errors, the QoS requirements are usually implied by probabilistic SINR constraints as in [20]–[22], or in terms of equivalent rate-outage probability constraints [23]–[25]. Given in either form, the stochastically robust schemes mostly apply the robust (chance-constrained) optimization techniques introduced in [26] and [27] in order to deal with the design problem.

Robust design of symbol-level precoding (SLP) is not well investigated in the literature. Worst-case robust approaches are proposed in [28] and [29] for unsecured and secured wireless systems, respectively, aiming to design the symbol-level precoder with norm-bounded CSI errors based on power minimization and max-min fairness criteria. It is, however, important to notice that as far as the symbol-level power minimization problem is concerned, the norm-bounded uncertainty model might not yield an efficient solution. This modeling ultimately leads to a worst-case conservatism which inherently increases the transmission power, though enhancing the users' received SINR and symbol error probability. To the best of the authors' knowledge, there is no published work to date with the aim of developing a stochastically robust symbol-level design formulation. It is worth mentioning that a precoding optimization problem with outage probability constraints based on a symbol-level approach is presented in [30], therein the goal is to achieve robustness to the receiver noise, but not to any type of channel uncertainties.

In this paper, we address the problem of SLP design in the presence of channel uncertainty. Our goal is to optimize the (total) transmission power under joint CI and SINR constraints. In the optimization problem, the CI constraints are formulated based on the definition of distance-preserving constructive interference regions introduced in [31]. Considering a stochastic uncertainty model, in order to obtain a robust formulation for the original CI constraints, it is essential to characterize the uncertain component in the CI inequality which appears as a result of the imperfect available CSI. Our primary challenge, however, is to obtain a tractable (deterministic) convex approximation for the probabilistic robust formulation, ensuring that the desired constraint is met with a certain probability for any realization of the CSI error within the uncertainty set. In such a conservative approach, the relative tightness of the derived approximations, which (roughly speaking) measures the cost of tractability, will be of particular importance. Having the convex robust constraints, the subsequent modification of the precoding design problem is straightforward due to the fact that the only uncertain part of the problem is the set of CI constraints. Accordingly, the main contributions of this paper are listed as below:

1. We propose some modifications to the CI constraints according to a stochastic (Gaussian) uncertainty model. In particular, we redefine the CI constraints as chance-constrained inequalities for which we derive two deterministic convex robust alternatives based on the notion of safe approximation. Both approximations are formulated as convex second-order cone constraints, hence can efficiently be handled. We further obtain a third robust CI restriction as our benchmark for comparison, which is based on the well known idea of sphere bounding. We then compare the relative tightness of the obtained robust approximations analytically and validate the discussion through simulation results. Our results indicate that the proposed robust approaches provide tighter approximations than the sphere bounding based method.
2. Using the robust safe approximations of CI constraints, we propose robust design formulations in the form of convex second-order cone program (SOCP) for the QoS-constrained (symbol-level) power minimization problem. We then analyze and compare the computational complexities of the robust and non-robust precoding schemes, thereby indicating that the proposed robust approaches have higher computational cost (by a limiting order of the number of users) compared to the original non-robust problem, .

**Organization:** The rest of this paper is organized as follows. We describe the system and uncertainty models in Section II. In Section III, first we briefly explain the original SLP problem with non-robust CI constraints. We then define probabilistic robust counterparts for the CI constraints and derive new formulations in the form of approximate convex restrictions in Section IV, which is followed by analytic discussions on the tightness of these approximations. In Section V, we cast the robust SLP optimization problem and analyze the computational complexity. Our simulation results are provided in Section VI. Finally, we conclude the paper in Section VII.
**Notations:** We use uppercase and lowercase bold-faced letters to denote matrices and vectors, respectively. The sets of real and complex numbers are represented by $\mathbb{R}$ and $\mathbb{C}$. For a complex input, $\mathrm{Re}\{\cdot\}$ and $\mathrm{Im}\{\cdot\}$ respectively denote real and imaginary parts. For matrices and vectors, $[\,\cdot\,]^T$ denotes transpose. For a (square) matrix $\mathbf{A}$, $|\mathbf{A}|$ and $\mathrm{Tr}(\mathbf{A})$ respectively denote the determinant and the trace of $\mathbf{A}$, $\mathrm{vec}(\mathbf{A})$ stands for the vector obtained by stacking the columns of $\mathbf{A}$, and $\mathbf{A} \succeq 0$ (or $\mathbf{A} \preceq 0$) means that $\mathbf{A}$ is positive semidefinite (or negative semidefinite). For two square matrices $\mathbf{A}$ and $\mathbf{B}$ with identical dimensions, $\mathbf{A} \succeq \mathbf{B}$ means $\mathbf{A} - \mathbf{B}$ is positive semidefinite. Given two vectors $\mathbf{x} \in \mathbb{R}^n$ and $\mathbf{y} \in \mathbb{R}^n$, $\mathbf{x} \geq \mathbf{y}$ (or $\mathbf{x} \ngeq \mathbf{y}$) denotes the entrywise inequality. $\|\cdot\|_2$ and $\|\cdot\|_F$ represent the vector Euclidean norm and the matrix Frobenius norm, respectively. $\mathbf{I}$, $\mathbf{0}$ and $\mathbf{1}$ respectively stand for the identity matrix, the zero matrix (or the zero vector, depending on the context) and the all-one vector of appropriate dimension. The probability function and the statistical expectation are respectively denoted by $\mathbb{P}\{\cdot\}$ and $\mathbb{E}\{\cdot\}$. The operators $\otimes$ and $\circ$ stand for the Kronecker and the Hadamard products, respectively.

## II. System and Uncertainty Model

We consider an MU-MISO wireless broadcast channel in which a common transmitter (e.g., a base station), equipped

with $N$ antennas, serves $K$ single-antenna users by sending independent data streams, where $K \leq N$. We denote by the row vector $\mathbf{h}_k \in \mathbb{C}^{1\times N}, k = 1, ..., K$, the instantaneous (frequency-flat) fading channel of the $k$th transmit/receive antenna pair. In the downlink transmission, at any symbol time $t = 0, 1, 2, ...$, independent data symbols $s_k(t), k = 1, ..., K$, are to be conveyed to the users, with $s_k(t)$ denoting the intended symbol for the $k$th user. To simplify the notation, we focus on a specific symbol time and drop the time index $t$ throughout the paper. Each symbol $s_k$ is drawn from a finite equiprobable constellation set with unit average power. We confine ourselves to constellation sets with unbounded (Voronoi) decision regions, including single-level modulation schemes, e.g., phase-shift keying (PSK). We further assume, without loss of generality, identical modulation schemes for all the users.

We collect the intended symbols for all $K$ users in a vector denoted by $\mathbf{s} = [s_1, \ldots, s_K]^T \in \mathbb{C}^{K\times 1}$. The symbol vector $\mathbf{s}$ is then mapped to $N$ transmit antennas yielding the transmit vector $\mathbf{u} = [u_1, \ldots, u_N]^T \in \mathbb{C}^{N\times 1}$. This mapping is done with the use of an appropriately designed multiuser precoding module. In this paper, we adopt a symbol-level precoding (SLP) scheme based on a particular type of constructive interference regions, which will be discussed in more detail later. It is worth noting that unlike conventional (block-level) linear precoding schemes, e.g., (regularized) zero-forcing or minimum mean square error, the nonlinear-precoded signal $\mathbf{u}$ might not be explicitly decomposed as a linear combination of distinct users' signatures (i.e., precoding vectors). Instead, the optimal transmit signal $\mathbf{u}$ is obtained as a result of an objective-oriented precoding design on a symbol-by-symbol basis. Under the above assumptions, the baseband representation of the received signal at the receiver of the $k$th user is given by

$$r_k = \mathbf{h}_k\mathbf{u} + z_k,\ k = 1, ..., K, \tag{1}$$

where $z_k$ denotes the additive circularly symmetric complex Gaussian noise with distribution $z_k \sim \mathcal{CN}(0, \sigma_k^2)$. At the receiver side, the $k$th user may use the conventional optimal single-user detector based on a maximum-likelihood (ML) decision rule to detect its intended symbol $s_k$, i.e., the structure of the receiver is independent of the precoder design.

While it is assumed that all the users have perfect knowledge of their own channels, the transmitter normally has inaccurate CSI due to several reasons such as imperfect channel estimation, limited (or delayed) feedback and quantization errors. By adopting a perturbation-based uncertainty model, the actual channel of user $k$ can be expressed as

$$\mathbf{h}_k = \hat{\mathbf{h}}_k + \mathbf{e}_k,\ k = 1, ..., K, \tag{2}$$

where $\hat{\mathbf{h}}_k \in \mathbb{C}^{1\times N}$ is the erroneous channel of user $k$ and $\mathbf{e}_k \in \mathbb{C}^{1\times N}$ represents the additive CSI error, while only $\hat{\mathbf{h}}_k$ is assumed to be known to the transmitter. The actual channel $\mathbf{h}_k$, the estimate channel $\hat{\mathbf{h}}_k$, and the CSI error vector $\mathbf{e}_k$ are assumed to be mutually uncorrelated for all $k = 1, ..., K$. We consider a stochastic uncertainty model according to which the channel error vectors are distributed as $\mathbf{e}_k \sim \mathcal{CN}(\mathbf{0}, \xi_k^2\mathbf{I})$ for all $k = 1, ..., K$, where $\xi_k^2$ denotes the variance of the CSI error and is assumed to be available at the transmitter. Note that the available channel $\hat{\mathbf{h}}_k$ can be viewed as the estimated channel resulting from an imperfect estimation process, while $\mathbf{e}_k$ captures the Gaussian estimation error. In general, the error variance $\xi_k^2$ depends on the quality of the estimated channel and the imperfections in the estimation process. The stochastic error model specifically corresponds to time-division duplex systems, where the transmitter exploits the estimated uplink channel for the downlink precoding [21]. It is worth noting that the uncertainty model (2) may also appear in a different scenario with statistical CSI where the channel statistics are assumed to be (partially) known at the transmitter, e.g., either the channel's mean or covariance (or both) is (are) available; see, e.g., [20], [32], [33]. In such a case, one may model the statistical CSI as $\mathbf{h}_k \sim \mathcal{CN}(\hat{\mathbf{h}}_k, \xi_k^2\mathbf{I})$, which ultimately leads to similar results.

From now on, it is more convenient to use equivalent real-valued notations instead of the complex-valued ones, i.e.,

$$\tilde{\mathbf{u}} = \begin{bmatrix}\mathrm{Re}(\mathbf{u})\\ \mathrm{Im}(\mathbf{u})\end{bmatrix} \in \mathbb{R}^{2N\times 1}, \mathbf{s}_k = \begin{bmatrix}\mathrm{Re}(s_k)\\ \mathrm{Im}(s_k)\end{bmatrix} \in \mathbb{R}^2, k = 1, ..., K.$$

Furthermore, by defining the operator

$$\mathrm{T}(\mathbf{x}) \triangleq \begin{bmatrix}\mathrm{Re}(\mathbf{x}) & -\mathrm{Im}(\mathbf{x})\\ \mathrm{Im}(\mathbf{x}) & \mathrm{Re}(\mathbf{x})\end{bmatrix},$$

for any given complex vector $\mathbf{x}$, we denote

$$\mathbf{H}_k = \mathrm{T}(\mathbf{h}_k),\ \hat{\mathbf{H}}_k = \mathrm{T}(\hat{\mathbf{h}}_k),\ \mathbf{E}_k = \mathrm{T}(\mathbf{e}_k),\ k = 1, ..., K,$$

where all the above defined matrices belong to $\mathbb{R}^{2\times 2N}$. From the newly introduced notations, it is immediately apparent that

$$\mathbf{H}_k = \hat{\mathbf{H}}_k + \mathbf{E}_k,\ k = 1, ..., K. \tag{3}$$

and

$$\mathbf{H}_k\tilde{\mathbf{u}} = \begin{bmatrix}\mathrm{Re}(\mathbf{h}_k\mathbf{u})\\ \mathrm{Im}(\mathbf{h}_k\mathbf{u})\end{bmatrix}. \tag{4}$$

Note also that $\mathbf{E}_k(j,:) \sim \mathcal{N}(\mathbf{0},\ \frac{1}{2}\xi_k^2\mathbf{I}), k = 1, ..., K, j = 1, 2$, where $\mathbf{E}_k(j,:)$ refers to the $j$th row of $\mathbf{E}_k$. In the rest of this paper, we unify the norm notations such that $\|\cdot\|$ denotes either the Frobenius norm of a matrix or the Euclidean norm of a vector. In addition, for each user $k = 1, ..., K$, by "received signal" we mean the noise-free received signal, i.e., $\mathbf{H}_k\tilde{\mathbf{u}}$.

## III. SINR-Constrained SLP Power Minimization

A crucial design consideration for SLP is to accommodate the received signal of each user $k$ into a pre-specified region, called constructive interference (CI) region, corresponding to the intended symbol $s_k$. The CI regions, which are modulation-specific regions, have been defined in several ways in the literature; see, e.g., [8], [28], [31]. As mentioned earlier, we focus on the so-called distance-preserving CI regions [31], which are defined in a generic form that is applicable to any given (two-dimensional) modulation scheme.

In order to design the symbol-level precoder, we are particularly interested in an SINR-constrained power minimization problem. Let us, for the moment, assume that the downlink channels are perfectly known to the transmitter, i.e., $\hat{\mathbf{H}}_k = \mathbf{H}_k$ for all $k = 1, ..., K$. In this perfect CSI case, it has been shown

in [34] that the design problem of interest can be expressed as

$$\mathcal{P}1: \quad \underset{\tilde{\mathbf{u}}}{\text{minimize}} \quad \tilde{\mathbf{u}}^T\tilde{\mathbf{u}} \quad \text{s.t.} \quad \mathbf{A}_k\mathbf{H}_k\tilde{\mathbf{u}} \geq \sigma_k\sqrt{\gamma_k}\,\mathbf{A}_k\mathbf{s}_k,\ k=1,...,K, \tag{5}$$

where $\mathbf{A}_k\mathbf{H}_k\tilde{\mathbf{u}} \geq \sigma_k\sqrt{\gamma_k}\,\mathbf{A}_k\mathbf{s}_k$ refers to the CI constraint for the $k$th user. Further, $\mathbf{A}_k \in \mathbb{R}^{2\times 2}$ describes the distance-preserving region associated with $\mathbf{s}_k$ (notice that each symbol $\mathbf{s}_k$ corresponds to a constellation point), and $\gamma_k$ denotes the given SINR requirement of user $k$. Note that each matrix $\mathbf{A}_k$ contains the normal vectors of the two ML decision boundaries of symbol $\mathbf{s}_k$. More details on the formulation of distance-preserving CI regions as in (5) can be found in [34], [35].

The SLP design formulation in (5) aims to minimize the total (per-symbol) transmit power while satisfying certain CI constraints and given target SINRs $\gamma_k$ for all $K$ users. In the presentation of the design problem $\mathcal{P}1$, it is assumed that all the users' channels are perfectly known to the transmitter. However, with imperfect CSI, the design constraints are no longer guaranteed by the optimal solution of $\mathcal{P}1$. To be more specific, in case $\hat{\mathbf{H}}_k \neq \mathbf{H}_k$, the region described by $\mathbf{A}_k\hat{\mathbf{H}}_k\tilde{\mathbf{u}} \geq \sigma_k\sqrt{\gamma_k}\,\mathbf{A}_k\mathbf{s}_k$ is a distorted version of the accurate CI region. Consequently, a received signal $\mathbf{H}_k\tilde{\mathbf{u}}$ is no longer guaranteed to lie within the desired CI region, which may cause severe performance degradation. Further to this error-induced distortion of the CI regions, the users might not be provided with the minimum required SINRs given by the target values $\gamma_k, k = 1,...,K$. Therefore, having a robust formulation for the symbol-level precoding design problem is essential in order to ensure the CI constraints as well as the minimum SINR requirements of the users in any realizable case of the statistically known CSI. To this end, one first needs to properly reformulate the CI constraints in accordance with the uncertainty model.

## IV. Stochastic Robust CI Formulation

We start off by restating the accurate CI constraint to be met for user $k$, i.e.,

$$\mathbf{A}_k\mathbf{H}_k\tilde{\mathbf{u}} \geq \sigma_k\sqrt{\gamma_k}\mathbf{A}_k\mathbf{s}_k,\ k=1,...,K,$$

By substituting (3) for $\mathbf{H}_k$, we have

$$\mathbf{A}_k\hat{\mathbf{H}}_k\tilde{\mathbf{u}} \geq \sigma_k\sqrt{\gamma_k}\mathbf{A}_k\mathbf{s}_k - \mathbf{A}_k\mathbf{E}_k\tilde{\mathbf{u}},\ k=1,...,K. \tag{6}$$

A stochastic robust CI constraint must satisfy (6) with a certain probability for any possible realization of the CSI error $\mathbf{E}_k$ within the uncertainty region. Assuming statistically known CSI errors, the CI constraint in (6) turns into an uncertain inequality with the uncertainty arising from the stochastic CSI error $\mathbf{E}_k$. Although the feasible set of this uncertain inequality is always convex, the major difficulty is to efficiently check whether this convex constraint is satisfied at a given point, which is highly computationally demanding. In such a case, the (deterministic) constraint in (6) can be reformulated as a probabilistic constraint (commonly known as chance constraint). The chance constraint then implies that the $k$th user will experience the event of CI failure only with a constrained small probability, i.e.,

$$\mathbb{P}\left\{\mathbf{A}_k\hat{\mathbf{H}}_k\tilde{\mathbf{u}} \not\geq \sigma_k\sqrt{\gamma_k}\mathbf{A}_k\mathbf{s}_k - \mathbf{A}_k\mathbf{E}_k\tilde{\mathbf{u}}\right\} < \upsilon, \tag{7}$$

which can be equally expressed as

$$\mathbb{P}\left\{\mathbf{A}_k\hat{\mathbf{H}}_k\tilde{\mathbf{u}} \geq \sigma_k\sqrt{\gamma_k}\mathbf{A}_k\mathbf{s}_k - \mathbf{A}_k\mathbf{E}_k\tilde{\mathbf{u}}\right\} \geq 1-\upsilon, \tag{8}$$

where $\upsilon \in (0, 1/2]$ denotes the violation probability threshold which is a system design parameter controlling the desired level of conservatism. Remark that the SINR requirement $\gamma_k$ translates to an achievable target rate of $R_k = \log_2(1+\gamma_k)$, under ergodic conditions on the channel [36]. Therefore, the constraint (8) can also be read as a rate-outage probability constraint, ensuring that the transmission rate $R_k$ is achievable for the $k$th user with probability (at least) $1-\upsilon$. For the sake of notation, we denote the stochastic uncertain component of the CI constraint by

$$\mathbf{q}_k \triangleq \mathbf{A}_k\mathbf{E}_k\tilde{\mathbf{u}} = (\tilde{\mathbf{u}}^T \otimes \mathbf{A}_k)\,\mathrm{vec}(\mathbf{E}_k), \tag{9}$$

which can be simply verified using the well-known property $\mathrm{vec}(\mathbf{XYW}) = (\mathbf{W}^T \otimes \mathbf{X})\,\mathrm{vec}(\mathbf{Y})$, for any given matrices $\mathbf{X}, \mathbf{Y}, \mathbf{W}$ with appropriate dimensions, along with the fact that $\mathbf{A}_k\mathbf{E}_k\tilde{\mathbf{u}} = \mathrm{vec}(\mathbf{A}_k\mathbf{E}_k\tilde{\mathbf{u}})$. Let $\mathbf{A}_k = [\mathbf{a}_{k,1}, \mathbf{a}_{k,2}]^T$, then using (9), we can write

$$\mathbf{q}_k = \begin{bmatrix}(\tilde{\mathbf{u}}^T \otimes \mathbf{a}_{k,1}^T)\,\mathrm{vec}(\mathbf{E}_k)\\ (\tilde{\mathbf{u}}^T \otimes \mathbf{a}_{k,2}^T)\,\mathrm{vec}(\mathbf{E}_k)\end{bmatrix} \triangleq \begin{bmatrix}q_{k,1}\\ q_{k,2}\end{bmatrix}, \tag{10}$$

from which is clear that $\mathbf{q}_k$ is a bivariate (correlated) Gaussian random variable. We further denote the certain part of the CI inequality (6) by

$$\mathbf{w}_k(\tilde{\mathbf{u}}) \triangleq \sigma_k\sqrt{\gamma_k}\mathbf{A}_k\mathbf{s}_k - \mathbf{A}_k\hat{\mathbf{H}}_k\tilde{\mathbf{u}}, \tag{11}$$

which is affine in $\tilde{\mathbf{u}}$, where $\mathbf{w}_k(\tilde{\mathbf{u}}) = [w_{k,1}, w_{k,2}]^T$. Using the new notations, the chance constraint (8) can then be written, in a simpler form, as

$$\mathbb{P}\left\{\mathbf{q}_k \geq \mathbf{w}_k(\tilde{\mathbf{u}})\right\} \geq 1-\upsilon,\ k=1,...,K. \tag{12}$$

The constraints in (12) belong to chance-constrained vector inequalities, which are generally known to be computationally intractable [26], as we will also see later. In what follows, the goal is to derive equivalent deterministic expressions for (12). For this purpose, we first need to study the statistical properties of the uncertain vector $\mathbf{q}_k$.

We begin with the Gaussian error vector $\mathrm{vec}(\mathbf{E}_k)$ of which the mean and the covariance matrix are respectively given by $\mathbb{E}\{\mathrm{vec}(\mathbf{E}_k)\} = \mathbf{0}$ and

$$\mathbb{E}\left\{\mathrm{vec}(\mathbf{E}_k)\mathrm{vec}(\mathbf{E}_k)^T\right\} = \frac{1}{2}\,\xi_k^2\begin{bmatrix}\mathbf{I}_{2N} & \mathbf{J}\\ \mathbf{J}^T & \mathbf{I}_{2N}\end{bmatrix}, \tag{13}$$

where

$$\mathbf{J} = \mathbf{I}_N \otimes \mathbf{J}_2,\ \mathbf{J}_2 \triangleq \begin{bmatrix}0 & 1\\ -1 & 0\end{bmatrix}.$$

From (9), it is straightforward to show that $\mathbf{q}_k$ is a (possibly correlated) Gaussian random vector with mean

$$\mathbb{E}\{\mathbf{q}_k\} = \left(\tilde{\mathbf{u}}^T \otimes \mathbf{A}_k\right)\,\mathbb{E}\left\{\mathrm{vec}(\mathbf{E}_k)\right\} = \mathbf{0}, \tag{14}$$

and covariance

$$\begin{aligned}\mathbf{C}_k &= \mathbb{E}\{\mathbf{q}_k\mathbf{q}_k^T\} \\ &\overset{(a)}{=} (\tilde{\mathbf{u}}^T \otimes \mathbf{A}_k)\, \mathbb{E}\Big\{\mathrm{vec}(\mathbf{E}_k)\mathrm{vec}(\mathbf{E}_k)^T\Big\}(\tilde{\mathbf{u}} \otimes \mathbf{A}_k^T) \\ &\overset{(b)}{=} \frac{1}{2}\,\xi_k^2\,\left(\tilde{\mathbf{u}}^T\tilde{\mathbf{u}} \otimes \mathbf{A}_k\mathbf{A}_k^T\right) = \frac{1}{2}\,\xi_k^2\,\|\tilde{\mathbf{u}}\|^2\,\mathbf{A}_k\mathbf{A}_k^T,\end{aligned} \tag{15}$$

where the equality (a) can be verified using the property $(\mathbf{X}\otimes\mathbf{Y})^T = (\mathbf{X}^T\otimes\mathbf{Y}^T)$, for any given matrices $\mathbf{X},\mathbf{Y},\mathbf{W},\mathbf{Z}$, and the equality (b) has been verified in Appendix A.

**Remark 1.** Using the fact that $\mathbf{q}_k$ has a symmetric distribution around zero, it is trivial to verify that the chance constraint (12) is feasible for every $\upsilon \in (0, 1/2]$ if and only if (iff) we have $\mathbb{E}\{\mathbf{q}_k\} \geq \mathbf{w}_k(\tilde{\mathbf{u}})$. Therefore, under the assumption $\upsilon \in (0, 1/2]$, a necessary and sufficient condition for (12) to have a nonempty feasible region is $\mathbf{w}_k(\tilde{\mathbf{u}}) \leq \mathbf{0}$. For every $k \in \{1, ..., K\}$, this condition must be considered as a constraint in the formulation of the robust precoding optimization problem.

Using the first two moments of $\mathbf{q}_k$, the probability in (12) can be precisely evaluated as the integral of the joint Gaussian probability distribution of $q_{k,1}$ and $q_{k,2}$, i.e.,

$$\begin{aligned}\mathbb{P}\{\mathbf{q}_k \geq \mathbf{w}_k(\tilde{\mathbf{u}})\} &= \mathbb{P}\left\{q_{k,1} \geq w_{k,1}, q_{k,2} \geq w_{k,2}\right\} \\ &= \int_{w_{k,2}}^{\infty}\int_{w_{k,1}}^{\infty} \frac{1}{2\pi\sqrt{|\mathbf{C}_k|}}\exp\left\{-\frac{1}{2}\mathbf{q}_k^T\mathbf{C}_k^{-1}\mathbf{q}_k\right\}\mathrm{d}q_{k,1}\mathrm{d}q_{k,2}.\end{aligned} \tag{16}$$

However, no explicit closed-form expression is known for the integral in (16). It becomes even more challenging to imply the constraint (16) in the precoding optimization problem. In order to resolve the difficulty of finding a tractable (convex) expression for (16), a straightforward approach is to eliminate the (possible) correlation between the entries of $\mathbf{q}_k$ through applying a whitening transform. In this regard, the optimal whitening matrix (in the sense of minimum mean-square error) is shown in [37] to be

$$\mathbf{C}_k^{-1/2} = \frac{\sqrt{2}}{\xi_k\,\|\tilde{\mathbf{u}}\|}\,(\mathbf{A}_k\mathbf{A}_k^T)^{-1/2}, \tag{17}$$

where $(\cdot)^{-1/2}$ denotes the inverse square root. It is worthwhile to mention that in [34], the $2\times 2$ matrix $\mathbf{A}_k\mathbf{A}_k^T$ is proven to be always non-singular, and thus, $\mathbf{C}_k$ is positive definite and has a unique (invertible) square root. As a result, the probability expression in (16) can be equally written as

$$\begin{aligned}\mathbb{P}\left\{\mathbf{q}_k \geq \mathbf{w}_k(\tilde{\mathbf{u}})\right\} &= \mathbb{P}\left\{\mathbf{C}_k^{1/2}\mathbf{C}_k^{-1/2}\mathbf{q}_k \geq \mathbf{w}_k(\tilde{\mathbf{u}})\right\} \\ &= \mathbb{P}\left\{\bar{\mathbf{q}}_k \geq \mathbf{C}_k^{-1/2}\mathbf{w}_k(\tilde{\mathbf{u}})\right\} \\ &= \mathbb{P}\left\{\bar{\mathbf{q}}_k \geq \bar{\mathbf{w}}_k(\tilde{\mathbf{u}})\right\},\end{aligned} \tag{18}$$

where $\bar{\mathbf{q}}_k \triangleq \mathbf{C}_k^{-1/2}\mathbf{q}_k$ and $\bar{\mathbf{w}}_k(\tilde{\mathbf{u}}) \triangleq \mathbf{C}_k^{-1/2}\mathbf{w}_k(\tilde{\mathbf{u}})$. It can immediately be seen that $\bar{\mathbf{q}}_k$ is an uncorrelated zero-mean Gaussian random vector with unit diagonal covariance matrix, i.e.,

$$\begin{aligned}\bar{\mathbf{C}}_k &\triangleq \mathbb{E}\left\{\bar{\mathbf{q}}_k\bar{\mathbf{q}}_k^T\right\} \\ &= \mathbb{E}\left\{\mathbf{C}_k^{-1/2}\mathbf{q}_k\mathbf{q}_k^T\mathbf{C}_k^{-1/2}\right\} \\ &= \mathbf{C}_k^{-1/2}\mathbb{E}\left\{\mathbf{q}_k\mathbf{q}_k^T\right\}\mathbf{C}_k^{-1/2} \\ &= \mathbf{C}_k^{-1/2}\mathbf{C}_k\mathbf{C}_k^{-1/2} = \mathbf{I}.\end{aligned} \tag{19}$$

Consequently, the chance constraint (12) is equivalent to

$$\mathbb{P}\left\{\bar{\mathbf{q}}_k \geq \bar{\mathbf{w}}_k(\tilde{\mathbf{u}})\right\} \geq 1 - \upsilon, \tag{20}$$

with $\bar{\mathbf{q}}_k \sim \mathcal{N}(\mathbf{0}, \mathbf{I})$. This probability may appear to be easily handled as it can be expressed by the product of two (complementary) error functions. In the context of convex optimization, however, we essentially need to reach a convex representation for (20). This could be in general an intricate task since the joint probability in (20) does not admit a tractable convex expression. An alternative approach to tackle this intractability is to replace (20) with its *safe tractable approximation*, resulting in an efficiently computable convex constraint. Such an approximation lies within the literature of robust optimization techniques [26], [27]. The term *safe* is used here in the sense that the feasible points of the safe approximation must be necessarily feasible also for (20). Therefore, in what follows the goal is to propose computationally tractable (but possibly not equivalent) convex approximations implying the CI chance constraint (20).

**Remark 2.** Similar to Remark 1, since $\bar{\mathbf{q}}_k$ is symmetrically distributed around zero, the chance constraint (20) is feasible for $\upsilon \in (0, 1/2]$ iff $\mathbb{E}\{\bar{\mathbf{q}}_k\} \geq \bar{\mathbf{w}}_k(\tilde{\mathbf{u}})$, or equivalently iff $\bar{\mathbf{w}}_k(\tilde{\mathbf{u}}) \leq \mathbf{0}$. For practical modulation schemes, however, using the definition of $\bar{\mathbf{w}}_k(\tilde{\mathbf{u}})$, one can verify that the condition $\mathbf{w}_k(\tilde{\mathbf{u}}) \leq \mathbf{0}$ is also sufficient to have $\bar{\mathbf{w}}_k(\tilde{\mathbf{u}}) \leq \mathbf{0}$; see [34].

### *A. Proposed Safe Approximation I*

One may simply exploit the fact that the two random entries of $\bar{\mathbf{q}}_k$ are uncorrelated, hence independent. Consequently, denoting $\bar{\mathbf{q}}_k = [\bar{q}_{k,1}, \bar{q}_{k,2}]^T$ and $\bar{\mathbf{w}}_k(\tilde{\mathbf{u}}) = [\bar{w}_{k,1}, \bar{w}_{k,2}]^T$, by using the Gaussian cumulative distribution function, the joint probability in (20) can be separated as

$$\begin{aligned}\mathbb{P}\left\{\bar{\mathbf{q}}_k \geq \bar{\mathbf{w}}_k(\tilde{\mathbf{u}})\right\} &= \mathbb{P}\left\{\bar{q}_{k,1} \geq \bar{w}_{k,1}\right\}\ \mathbb{P}\left\{\bar{q}_{k,2} \geq \bar{w}_{k,2}\right\} \\ &= \frac{1}{2}\mathrm{erfc}\left(\frac{\bar{w}_{k,1}}{\sqrt{2}}\right) \times \frac{1}{2}\mathrm{erfc}\left(\frac{\bar{w}_{k,2}}{\sqrt{2}}\right),\end{aligned} \tag{21}$$

where $\mathrm{erfc}(\cdot)$ is the complementary error function defined by $\mathrm{erfc}(z) \triangleq \frac{2}{\sqrt{\pi}}\int_z^{\infty} e^{-t^2}dt$. Due to the decreasing monotonicity of the complementary error function, the desired probability is always bounded from below by

$$\mathbb{P}\left\{\bar{\mathbf{q}}_k \geq \bar{\mathbf{w}}_k(\tilde{\mathbf{u}})\right\} \geq \frac{1}{4}\,\mathrm{erfc}^2\left(\frac{\max\{\bar{w}_{k,1}, \bar{w}_{k,2}\}}{\sqrt{2}}\right). \tag{22}$$

Using (22), in order to imply the chance constraint (20), it is sufficient to consider the deterministic constraint

$$\frac{1}{4}\,\mathrm{erfc}^2\left(\frac{\max\{\bar{w}_{k,1}, \bar{w}_{k,2}\}}{\sqrt{2}}\right) \geq 1 - \upsilon, \tag{23}$$

which can be written as

$$-\max\left[\bar{\mathbf{w}}_k(\tilde{\mathbf{u}})\right] \leq \rho(\upsilon), \tag{24}$$

where $\rho(\upsilon) \triangleq -\sqrt{2}\,\mathrm{erfc}^{-1}\left(2\sqrt{1-\upsilon}\right)$ with $\mathrm{erfc}^{-1}(\cdot)$ denoting the inverse complementary error function, and $\max[\cdot]$ denotes the elementwise maximum. It can be verified that the elementwise maximum of affine functions in (24) is convex; see [38, p. 80]. Therefore, replacing $\bar{\mathbf{w}}_k(\tilde{\mathbf{u}})$, the conservative robust

approximation (24) can be rewritten in the form of a convex second-order cone (SOC) constraint as

$$\text{A1}: \quad \|\tilde{\mathbf{u}}\| \leq \frac{-\sqrt{2}}{\rho(\upsilon)\,\xi_k} \max\left[(\mathbf{A}_k\mathbf{A}_k^T)^{-1/2}\mathbf{w}_k(\tilde{\mathbf{u}})\right], \quad (25)$$

It should be remarked that, in general, the feasible region of A1 is a convex subset of that of (20). Therefore, the convex approximation A1 may not exactly imply the desired chance constraint (20), but any feasible solution to (25) is guaranteed to be feasible also for (20).

### *B. Proposed Safe Approximation II*

Our subsequent derivation of a second safe tractable approximation for (20) is essentially based on the well-known Schur complement lemma and the following theorem [26, Th. 4.1].

**Lemma 1.** *(Schur complement) Let* $\mathbf{W}$ *be a symmetric matrix given by*

$$\mathbf{W} = \begin{bmatrix} \mathbf{X} & \mathbf{Y} \\ \mathbf{Y}^T & \mathbf{Z} \end{bmatrix}. \quad (26)$$

*Then,* $\mathbf{W} \succeq 0$ *if and only if* $\mathbf{X} \succeq 0$ *and* $\mathbf{\Delta}_{\mathbf{X}} \succeq 0$*, where* $\mathbf{\Delta}_{\mathbf{X}} = \mathbf{Z} - \mathbf{Y}^T\mathbf{X}^{-1}\mathbf{Y}$ *is the Schur complement of* $\mathbf{X}$ *in* $\mathbf{W}$*.*

**Theorem 2.** *Let* $\mathbf{\Sigma}_0, \mathbf{\Sigma}_1, ..., \mathbf{\Sigma}_L$ *be diagonal* $n \times n$ *matrices with* $\mathbf{\Sigma}_0 \succeq 0$*, and* $\zeta_1, ..., \zeta_L$ *be mutually independent random variables where* $\zeta_l \sim \mathcal{N}(0,1), \forall l \in \{1, ..., L\}$*. Then, the semidefinite constraint*

$$\text{Arw}\left(\mathbf{\Sigma}_0, \mathbf{\Sigma}_1, ..., \mathbf{\Sigma}_L\right) \succeq 0,$$

*implies, for every* $\upsilon \in (0, 1/2]$*, that*

$$\mathbb{P}\left\{-\psi(\upsilon)\mathbf{\Sigma}_0 \preceq \sum_{l=1}^{L} \zeta_l \mathbf{\Sigma}_l \preceq \psi(\upsilon)\mathbf{\Sigma}_0\right\} \geq 1 - \upsilon,$$

*with* $\psi(\upsilon) = \text{erfc}^{-1}\left(\frac{\upsilon}{2n}\right)$*, where*

$$\text{Arw}\left(\mathbf{\Sigma}_0, \mathbf{\Sigma}_1, ..., \mathbf{\Sigma}_L\right) \triangleq \begin{bmatrix} \mathbf{\Sigma}_0 & \mathbf{\Sigma}_1 & \mathbf{\Sigma}_2 & \cdots & \mathbf{\Sigma}_L \\ \mathbf{\Sigma}_1 & \mathbf{\Sigma}_0 & \mathbf{0} & \cdots & \mathbf{0} \\ \mathbf{\Sigma}_2 & \mathbf{0} & \mathbf{\Sigma}_0 & \cdots & \mathbf{0} \\ \vdots & \vdots & \vdots & \ddots & \vdots \\ \mathbf{\Sigma}_L & \mathbf{0} & \mathbf{0} & \cdots & \mathbf{\Sigma}_0 \end{bmatrix}.$$

We recall that our goal here is to find a tractable sufficient (convex) condition for the CI inequality in (20) to be satisfied with probability at least $1 - \upsilon$. The inequality of interest, i.e., $\bar{\mathbf{q}}_k \geq \bar{\mathbf{w}}_k(\tilde{\mathbf{u}})$, can be equivalently expressed by a linear matrix inequality (LMI) as

$$\psi(\upsilon)\mathbf{\Sigma}_{0,k} + \bar{q}_{k,1}\mathbf{\Sigma}_1 + \bar{q}_{k,2}\mathbf{\Sigma}_2 \succeq 0, \quad (27)$$

$$\mathbf{\Sigma}_{0,k} \triangleq \frac{1}{\psi(\upsilon)} \begin{bmatrix} -\bar{w}_{k,1} & 0 \\ 0 & -\bar{w}_{k,2} \end{bmatrix}, \mathbf{\Sigma}_1 \triangleq \begin{bmatrix} 1 & 0 \\ 0 & 0 \end{bmatrix}, \mathbf{\Sigma}_2 \triangleq \begin{bmatrix} 0 & 0 \\ 0 & 1 \end{bmatrix},$$

Since $\bar{q}_{k,1}$ and $\bar{q}_{k,2}$ are both symmetric in distribution and the violation probability $\upsilon$ is (typically) small, a sufficient condition for

$$\mathbb{P}\left\{\psi(\upsilon)\mathbf{\Sigma}_{0,k} + \bar{q}_{k,1}\mathbf{\Sigma}_1 + \bar{q}_{k,2}\mathbf{\Sigma}_2 \succeq 0\right\} \geq 1 - \upsilon, \quad (28)$$

is also sufficient for

$$\mathbb{P}\left\{-\psi(\upsilon)\mathbf{\Sigma}_{0,k} \preceq \bar{q}_{k,1}\mathbf{\Sigma}_1 + \bar{q}_{k,2}\mathbf{\Sigma}_2 \preceq \psi(\upsilon)\mathbf{\Sigma}_{0,k}\right\} \geq 1 - \upsilon. \quad (29)$$

By a direct application of Theorem 2 with $n = 2$ and $L = 2$, it follows that the chance constraint (29) is met if

$$\text{Arw}(\mathbf{\Sigma}_{0,k}, \mathbf{\Sigma}_1, \mathbf{\Sigma}_2) \succeq 0, \quad (30)$$

holds true with $\psi(\upsilon) = \text{erfc}^{-1}\left(\frac{\upsilon}{4}\right)$. Notice that a necessary condition for Theorem 2 to be valid is $\mathbf{\Sigma}_{0,k} \succeq 0$. The matrix $\text{Arw}(\mathbf{\Sigma}_{0,k}, \mathbf{\Sigma}_1, \mathbf{\Sigma}_2)$ is symmetric, and further, can be partitioned as required in (26). As a result, using Lemma 1 with $\mathbf{X} = \mathbf{\Sigma}_{0,k}$ and $\mathbf{W} = \text{Arw}(\mathbf{\Sigma}_{0,k}, \mathbf{\Sigma}_1, \mathbf{\Sigma}_2)$, it can be immediately verified that the following implication holds:

$$\text{Arw}(\mathbf{\Sigma}_{0,k}, \mathbf{\Sigma}_1, \mathbf{\Sigma}_2) \succeq 0 \implies \mathbf{\Sigma}_{0,k} \succeq 0. \quad (31)$$

Therefore, the safe convex constraint (30) sufficiently implies our desired chance constraint in (29). Finally, by replacing $\mathbf{\Sigma}_{0,k}$, $\mathbf{\Sigma}_1$ and $\mathbf{\Sigma}_2$ in (30), the safe convex approximation is obtained as the semidefinite constraint

$$\begin{bmatrix} -\frac{\bar{w}_{k,1}}{\psi(\upsilon)} & 0 & 1 & 0 & 0 & 0 \\ 0 & -\frac{\bar{w}_{k,2}}{\psi(\upsilon)} & 0 & 0 & 0 & 1 \\ 1 & 0 & -\frac{\bar{w}_{k,1}}{\psi(\upsilon)} & 0 & 0 & 0 \\ 0 & 0 & 0 & -\frac{\bar{w}_{k,2}}{\psi(\upsilon)} & 0 & 0 \\ 0 & 0 & 0 & 0 & -\frac{\bar{w}_{k,1}}{\psi(\upsilon)} & 0 \\ 0 & 1 & 0 & 0 & 0 & -\frac{\bar{w}_{k,2}}{\psi(\upsilon)} \end{bmatrix} \succeq 0. \quad (32)$$

It is routine to check that the LMI in (32) is not convex in the given form with respect to $\tilde{\mathbf{u}}$. Nevertheless, it has been shown in Appendix B that, using the implication $\mathbf{w}_k \leq \mathbf{0}$ provided in Remark 1, it is possible to recast the semidefinite constraint (32) as an equivalent SOC constraint given by

$$\text{A2}: \quad \|\tilde{\mathbf{u}}\|\,\mathbf{1} \leq \frac{-\sqrt{2}}{\psi(\upsilon)\,\xi_k}(\mathbf{A}_k\mathbf{A}_k^T)^{-1/2}\mathbf{w}_k(\tilde{\mathbf{u}}), \quad (33)$$

which is indeed convex in $\tilde{\mathbf{u}}$, and can efficiently be handled by standard convex optimization tools [38].

### *C. Sphere Bounding Method (Benchmark)*

In order to gain some insight into the proposed safe convex approximation A2, and further for comparison purposes, we also formulate a benchmark approximation based on the so-called sphere bounding method. The idea (in some sense) is borrowed from the worst-case robust design approach. More specifically, the goal is basically to find a bounded uncertainty set to which the stochastically uncertain component in (20) belongs with a certain probability; subsequently, the worst-case approach can be applied. The following lemma from [25] helps us to proceed with the formulation.

**Lemma 3.** *Let* $\mathcal{S} \subset \mathbb{R}^n$ *be an arbitrary set with the property* $f(\mathbf{x}) \geq \mathbf{0}, \forall \mathbf{x} \in \mathcal{S}$*, where* $f(\cdot)$ *is in general a vector-valued function. Then, for a given* $\mathbf{y} \in \mathbb{R}^n$*, the restriction*

$$\mathbb{P}\left\{f(\mathbf{y}) \geq \mathbf{0}\right\} \geq 1 - \upsilon,$$

*is implied sufficiently by satisfying* $\mathbb{P}\left\{\mathbf{y} \in \mathcal{S}\right\} \geq 1 - \upsilon$*.*

In order to imply the chance constraint (20), one may use the implication provided by Lemma 3 to obtain a (preferably) tight convex restriction, as long as the resulting constraint is

efficiently computable. This requires to properly choose the set $\mathcal{S} \subseteq \mathbb{R}^2$ in such a way that the condition

$$f(\bar{\mathbf{q}}_k) \geq \mathbf{0},\ f(\bar{\mathbf{q}}_k) \triangleq \bar{\mathbf{q}}_k - \bar{\mathbf{w}}_k(\tilde{\mathbf{u}}), \tag{34}$$

is met for all $\bar{\mathbf{q}}_k \in \mathcal{S}$, while satisfying $\mathbb{P}\{\bar{\mathbf{q}}_k \in \mathcal{S}\} \geq 1-\upsilon$. We recall that $\bar{\mathbf{q}}_k \sim \mathcal{N}(\mathbf{0}, \mathbf{I})$, and that $\bar{\mathbf{q}}_k$ has a symmetric distribution. Thus, the condition (34) can be equally expressed as

$$f(\bar{\mathbf{q}}_k) \leq \mathbf{0},\ f(\bar{\mathbf{q}}_k) \triangleq \bar{\mathbf{q}}_k + \bar{\mathbf{w}}_k(\tilde{\mathbf{u}}). \tag{35}$$

A common (convex) choice for the set $\mathcal{S}$ to reach a computationally tractable formulation is the ball represented by

$$\mathcal{S} \triangleq \left\{\mathbf{x} \in \mathbb{R}^2 : \|\mathbf{x}\| \leq \alpha(\upsilon)\right\}, \tag{36}$$

with a radius of

$$\alpha(\upsilon) = \sqrt{\Phi_2^{-1}(1-\upsilon)},$$

where $\Phi_n^{-1}(\cdot)$ is the inverse cumulative distribution function of the central Chi-square random variable with $n$ degrees of freedom. It is then straightforward to verify that

$$\mathbb{P}\{\bar{\mathbf{q}}_k \in \mathcal{S}\} = 1-\upsilon, \tag{37}$$

from which it can be presumed that $\bar{\mathbf{q}}_k$ is norm-bounded by $\alpha(\upsilon)$ with a probability of $1-\upsilon$. As a result,

$$\alpha(\upsilon)\mathbf{1} + \bar{\mathbf{w}}_k(\tilde{\mathbf{u}}) \leq \mathbf{0}, \tag{38}$$

implies that (35) holds true for all $\bar{\mathbf{q}}_k \in \mathcal{S}$. Finally, the worst-case robust approximation (38) can be expressed by an SOC constraint as

$$\mathrm{B}: \quad \|\tilde{\mathbf{u}}\|\,\mathbf{1} \leq \frac{-\sqrt{2}}{\alpha(\upsilon)\,\xi_k}(\mathbf{A}_k\mathbf{A}_k^T)^{-1/2}\mathbf{w}_k(\tilde{\mathbf{u}}). \tag{39}$$

In particular, the convex approximation $\mathcal{R}$ is able to control the radius $\alpha(\upsilon)$ according to the tolerable violation probability. It can immediately be inferred by comparing (33) and (39) that A2 resembles the sphere bounding based approximation B in form. Based on this resemblance, the safe approximation method for $\upsilon \in (0, 1/2]$ can be treated as defining the convex set $\mathcal{S}$ as a ball with a radius different from $\alpha(\upsilon)$, therefore with a different level of conservatism. In the next subsection, we compare the tightness of the proposed approximations with respect to the sphere bounding approach.

### *D. Relative Tightness Comparison*

Up until this point, we have derived deterministic tractable convex approximations that, though not exactly, sufficiently ensure the satisfaction of the robust CI constraint of interest. This tractability led us to sacrifice tightness with respect to the originally intractable chance constraint (20). It is therefore desirable to find the formulation provides the tightest approximation among all the other ones.

Having rather similar conic representations for the three stochastic robust CI constraints, which are summarized in Table I, enables us to compare the relative tightness of the derived convex approximations. Here, we specifically define the relative tightness from the transmit power point of view according to which a convex approximation is a tighter one if it admits lower optimal transmit powers $\|\tilde{\mathbf{u}}\|^2$. We use the following two lemmas in the sequel. The proofs are straightforward.

TABLE I
SUMMARY OF THE PROPOSED ROBUST CI FORMULATIONS.

| Method | Robust CI constraint ($k = 1, ..., K$) |
|---|---|
| Safe Approx. I | A1 : $\|\tilde{\mathbf{u}}\| \leq \frac{-\sqrt{2}}{\rho(\upsilon)\,\xi_k} \max\left[(\mathbf{A}_k\mathbf{A}_k^T)^{-1/2}\mathbf{w}_k(\tilde{\mathbf{u}})\right]$ with $\rho(\upsilon) = -\sqrt{2}\,\mathrm{erfc}^{-1}(2\sqrt{1-\upsilon})$ |
| Safe Approx. II | A2 : $\|\tilde{\mathbf{u}}\|\mathbf{1} \leq \frac{-\sqrt{2}}{\psi(\upsilon)\,\xi_k}(\mathbf{A}_k\mathbf{A}_k^T)^{-1/2}\mathbf{w}_k(\tilde{\mathbf{u}})$ with $\psi(\upsilon) = \mathrm{erfc}^{-1}\left(\frac{\upsilon}{4}\right)$ |
| Sphere Bounding | B : $\|\tilde{\mathbf{u}}\|\mathbf{1} \leq \frac{-\sqrt{2}}{\alpha(\upsilon)\,\xi_k}(\mathbf{A}_k\mathbf{A}_k^T)^{-1/2}\mathbf{w}_k(\tilde{\mathbf{u}})$ with $\alpha(\upsilon) = \sqrt{\Phi_2^{-1}(1-\upsilon)}$ |

**Lemma 4.** *Let $\tilde{\mathbf{u}}^*$ be feasible to*

$$\|\tilde{\mathbf{u}}\|\,\mathbf{1} \leq \frac{-\sqrt{2}}{\beta\,\xi_k}(\mathbf{A}_k\mathbf{A}_k^T)^{-1/2}\mathbf{w}_k(\tilde{\mathbf{u}}), \tag{40}$$

*with $\beta > 0$, and satisfy $\bar{\mathbf{w}}_k(\tilde{\mathbf{u}}^*) \leq \mathbf{0}$ as a necessary condition. Then, it is implied that*

$$\|\tilde{\mathbf{u}}^*\| \leq \frac{-\sqrt{2}}{\beta\,\xi_k}\max\left[(\mathbf{A}_k\mathbf{A}_k^T)^{-1/2}\mathbf{w}_k(\tilde{\mathbf{u}}^*)\right] \tag{41}$$

*where $\max[\,\cdot\,]$ is the entrywise maximum of an input vector.*

**Lemma 5.** *Consider the constraint*

$$\|\tilde{\mathbf{u}}\| \leq \frac{-\sqrt{2}}{\beta\,\xi_k}\max\left[(\mathbf{A}_k\mathbf{A}_k^T)^{-1/2}\mathbf{w}_k(\tilde{\mathbf{u}})\right]. \tag{42}$$

*where $\beta > 0$. Let $\tilde{\mathbf{u}}^*$ be feasible to* (42) *with $\beta = \beta_1 > 0$, then for any $\beta_1 \geq \beta_2 > 0$, the following chain of inequalities holds:*

$$\begin{aligned}\|\tilde{\mathbf{u}}^*\| &\leq \frac{-\sqrt{2}}{\beta_1\,\xi_k}\max\left[(\mathbf{A}_k\mathbf{A}_k^T)^{-1/2}\mathbf{w}_k(\tilde{\mathbf{u}}^*)\right] \\ &\leq \frac{-\sqrt{2}}{\beta_2\,\xi_k}\max\left[(\mathbf{A}_k\mathbf{A}_k^T)^{-1/2}\mathbf{w}_k(\tilde{\mathbf{u}}^*)\right],\end{aligned} \tag{43}$$

*which implies that $\tilde{\mathbf{u}}^*$ is feasible to* (42) *with $\beta = \beta_2$.*

It follows immediately from Lemma 4 and Lemma 5 that a relative comparison of the convex approximations A1, A2 and B reduces to just comparing $\rho(\upsilon)$, $\psi(\upsilon)$ and $\alpha(\upsilon)$. These three functions, however, depend on the violation probability $\upsilon$, as depicted in Fig. 1 for $\upsilon \in (0, 1/2]$. It can be observed from Fig. 1 that for small values of $\upsilon$ below $\sim 0.12$, which is of high practical interest, we have $\psi(\upsilon) \leq \rho(\upsilon) \leq \alpha(\upsilon)$. This means that a feasible solution to B is also feasible for A1 and A2, i.e., the optimal transmit power $\|\tilde{\mathbf{u}}^*\|^2$ obtained from A1 and A2 is no larger than that obtained from B. Therefore, the robust convex approximations A1 and A2 are tighter (hence less conservative) than our benchmark B. In a more precise order,

$$\mathcal{F}_{\mathrm{B}} \subseteq \mathcal{F}_{\mathrm{A1}} \subseteq \mathcal{F}_{\mathrm{A2}}, \tag{44}$$

where $\mathcal{F}_{(\cdot)}$ denotes the feasible region. It also follows from (44) that A2 is tighter than A1 in this range of $\upsilon$, i.e., under strict robustness settings. On the other hand, for higher values of $\upsilon$ up to $1/2$, which can be regarded as relaxed robustness

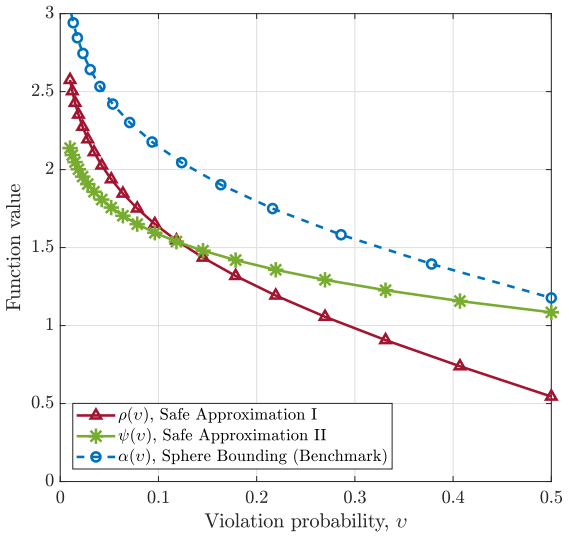


Fig. 1. Plot of $\rho(\upsilon)$, $\alpha(\upsilon)$ and $\psi(\upsilon)$ as a function of the violation probability.

conditions (but of course might be of less importance in a real system), we have $\rho(\upsilon) \leq \psi(\upsilon) \leq \alpha(\upsilon)$. This implies that A1 provides a tighter convex approximation than A2 in the high violation probability regime, but still A2 is tighter than the benchmark approximation.

## V. Robust SLP Optimization Problem

We formulate robust optimization problems for the power minimizing symbol-level precoder using the proposed robust implications of the CI constraints obtained in the previous section. First, recall the original (non-robust) formulation of the SLP design problem in (5). By introducing a slack variable $p \geq 0$, it is further possible to recast (5) as

$$\begin{aligned} \mathcal{P}1: \ \underset{\tilde{\mathbf{u}},p\geq 0}{\text{minimize}} \quad & p \\ \text{s.t.} \quad & \mathbf{A}_k\mathbf{H}_k\tilde{\mathbf{u}} \geq \sigma_k\sqrt{\gamma_k}\,\mathbf{A}_k\mathbf{s}_k, \ k=1,...,K, \\ & \tilde{\mathbf{u}}^T\tilde{\mathbf{u}} \leq p, \end{aligned} \tag{45}$$

which is a more convenient form for the subsequent computational complexity discussion in this section.

On the other hand, the robust counterpart of $\mathcal{P}1$ can simply be expressed by replacing the actual CI constraints with any of the robust constraints A1, A2, or B for all the users, i.e., all $K$ CI constraints must be implied through same type of convex restrictions. For instance, by adopting safe approximations of type A2, the resulting stochastic robust design formulation can be expressed as

$$\begin{aligned} \mathcal{P}2: \ \underset{\tilde{\mathbf{u}},p\geq 0}{\text{minimize}} \quad & p \\ \text{s.t.} \quad & \|\tilde{\mathbf{u}}\|\mathbf{1} \leq \frac{-\sqrt{2}}{\psi(\upsilon)\,\xi_k}(\mathbf{A}_k\mathbf{A}_k^T)^{-1/2}\mathbf{w}_k(\tilde{\mathbf{u}}), \\ & \mathbf{w}_k(\tilde{\mathbf{u}}) \leq \mathbf{0}, \\ & \tilde{\mathbf{u}}^T\tilde{\mathbf{u}} \leq p, \end{aligned} \tag{46}$$

The robust constraints A1, A2 and B, as summarized in Table I, can all be represented as second-order cone (SOC) constraints. Therefore, the robust optimization problem $\mathcal{P}2$ can be classified as a second-order cone programming (SOCP). It is, however, important to notice that while the non-robust formulation $\mathcal{P}1$ is always feasible, its robust counterpart $\mathcal{P}2$ may not share this property. To be more specific, there would be situations (e.g., with extremely small $\upsilon$ or large $\xi_k^2$) in which the robust CI constraints cannot all be satisfied with a finite transmit power $p$, meaning that the robust design is practically infeasible. In such cases, the intersection of all $K$ robust CI constraints would be an empty set.

*Computational Complexity Analysis:* We evaluate the computational complexity of the proposed robust design formulations based on the worst-case complexity analysis provided in [39], and compare the results with those of the original non-robust formulation. All the stochastic robust formulations are presented as SOCPs, which can efficiently be solved via interior-point methods. In general, the arithmetic complexity of a generic interior-point method entails the Newton complexity as well as per-iteration computation cost. The Newton complexity basically refers to the number of steps required to reduce the duality gap by a constant factor, while the per-iteration complexity involves finding a new search direction at each step, and is subsequently dominated by the computation effort to assemble and solve a linear system of equations. In particular, we briefly overview the complexity bound for an SOCP given in a generic form containing linear and (conic) quadratic constraints, to reach an $\epsilon$-solution (i.e., an $\epsilon$-optimal feasible solution) via a generic interior-point method.

For the second-order cone program

$$\begin{aligned} \underset{\mathbf{x}}{\text{minimize}} \quad & \mathbf{c}_0^T\mathbf{x} \\ \text{s.t.} \quad & \|\mathbf{F}_i\mathbf{x}+\mathbf{b}_i\| \leq \mathbf{f}_i^T\mathbf{x}+g_i, \ i=1,...,m, \\ & \mathbf{c}_j^T\mathbf{x} \leq d_j, \ j=1,...,l, \end{aligned} \tag{47}$$

where $\mathbf{F}_i \in \mathbb{R}^{n_i\times n}, \mathbf{b}_i \in \mathbb{R}^{n_i}, \mathbf{f}_i \in \mathbb{R}^n, g_i \in \mathbb{R}$ for all $i=0,1,...,m$, and $\mathbf{c}_j \in \mathbb{R}^n, d_j \in \mathbb{R}$ for $j=1,...,l$, the complexity bound of an $\epsilon$-solution is of order

$$\mathcal{C}(\mathcal{P},\epsilon) = n\sqrt{l+2m}\left(n^2+l(n+1)+\sum_{i=1}^{m}n_i^2\right)\mathcal{O}(1). \tag{48}$$

In the SOCP formulation (47), $n$ can be read as the total number of optimization variables, and $n_i$ determines the size of the $i$th cone constraint, which is related to the dimension of the $i$th second-order cone, for all $i=1,...,m$. Notice that this generic form of SOCP encompasses also the non-robust formulation in (45). Based on the above analysis, we are able to analyze the complexity of the robust SOCP design formulation (46), and compare it to that of its non-robust counterpart in (45). We also remark that

i. There are two real-valued second-order cone constraints associated with each user.
ii. The slack variables $p$ in (46) can be merged into the vector $\tilde{\mathbf{u}}$, increasing the $i$th cone's dimension by one for all $i=1,...,m$.

TABLE II
COMPLEXITY COMPARISON OF THE NON-ROBUST AND THE PROPOSED ROBUST DESIGN APPROACHES.

| Design problem | Complexity order $\left[\times \ln(\frac{1}{\epsilon})\right]$ | Dominating term [as $N, K \to \infty$] |
|---|---|---|
| $\mathcal{P}1$ | $2\sqrt{2K+2}\,.\,\mathcal{O}\left((2N+1)^3 + 2K(N+1)(2N+1)\right)$ | $\sqrt{K}\,.\,\mathcal{O}\left(N^3\right)\ln(\frac{1}{\epsilon})$ |
| $\mathcal{P}2$ | $2\sqrt{6K+2}\,.\,\mathcal{O}\left((K+1)(2N+1)^3 + 2K(2N+1)(N+1)\right)$ | $K\sqrt{K}\,.\,\mathcal{O}\left(N^3\right)\ln(\frac{1}{\epsilon})$ |

Accordingly, for all design problems, the number of variables is equal to $2N+1$. The non-robust formulation (45) has $2K+1$ linear inequalities plus one cone constraint of size $2N+1$, while the robust design formulation (46) involves $2K$ conic constraints of size $2N$ and one conic constraint of size $2N+1$ which corresponds to the power constraint. In Table II, the final complexity results obtained from (47) are reported, where the dominating terms represent the largest complexity growth rate as $N, K \to \infty$ under the assumption $K \leq N$. It follows from Table II that for both design problems, the proposed robust formulations increase the computational complexity of precoding design by an order of $\mathcal{O}(K)$, compared to that of their non-robust counterpart. Nonetheless, the increase in complexity is negligible for practical values of $K$.

## VI. SIMULATION RESULTS

In this section, we present our simulation results to evaluate the performance of the proposed robust SLP schemes, and further to validate the analytic discussions provided in earlier sections. The optimization problems have been solved using MATLAB software and SeDuMi solver [40]. The following setup is adopted in all the simulation scenarios. We consider a downlink multiuser MISO system with $N = 6$ and $K = 4$, employing an 8PSK modulation scheme with uncoded transmission. For all the users $k = 1, ..., K$, we assume unit noise variances $\sigma_k^2 \triangleq \sigma^2 = 1$ and equal SINR requirements $\gamma_k \triangleq \gamma$. The erroneous channel vectors $\{\hat{\mathbf{h}}_k\}_{k=1}^K$ are randomly generated according to a zero-mean unit variance circularly symmetric complex Gaussian distribution, where the channels of any two distinct users are uncorrelated, i.e., $\mathbb{E}\{\hat{\mathbf{h}}_k^H \hat{\mathbf{h}}_j\} = \mathbf{0}, \forall k, j = 1, ..., K, k \neq j$. We consider identical uncertainty regions for all the channels, i.e., $\xi_k^2 \triangleq \xi^2, k = 1, ..., K$. All the presented simulation results have been averaged over 500 fading block realizations, each of 500 symbols. We evaluate the performance of the symbol-level precoded downlink transmission under stochastically known CSI errors through various measures. The SLP approaches with robust CI constraints "safe approximation I", "safe approximation II", and "sphere bounding" are referred to as SA1-SLP, SA2-SLP and SB-SLP, respectively.

In Fig. 2, a scatter plot of the noise-free received signals is shown for the non-robust and robust SLP schemes. The average transmission powers for the non-robust SLP scheme with erroneous CSI and the robust SA2-SLP approach are 13.22 dBW and 15.08 dBW, respectively. It can be observed from the figure that this $\sim 2$ dBW extra power is consumed to satisfy the CI constraints with the given violation probability, thereby providing more safety to the subsequent additive Gaussian noise. The cloud of received signals corresponding

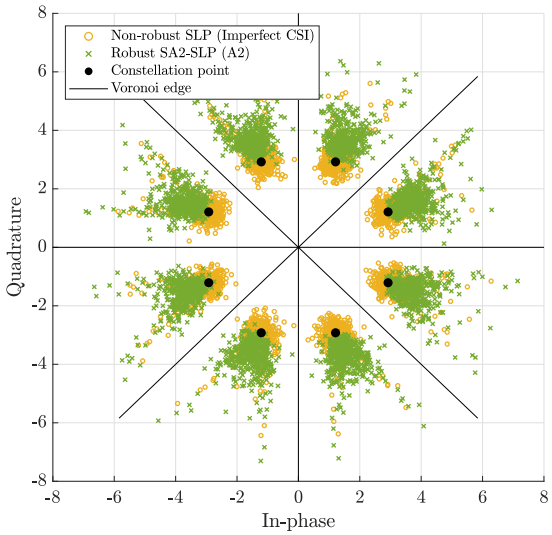


Fig. 2. Scatter plot of the noise-free received signals for 1000 trials with a fixed channel, $\gamma = 10$ dB, $\xi^2 = 0.005$ and $\upsilon = 0.05$.

to the non-robust SLP scheme, however, shows deviations from the intended symbols towards the corresponding ML decision boundaries, which may result in a higher symbol error probability (as we will see later in this section). Furthermore, the non-robust scheme may fail to satisfy the users' SINR requirements. This issue is depicted in Fig. 3 and Fig. 4, where we respectively plot the average per-user received SINR versus target SINR and the average received SINR for each user at a target value of $\gamma = 15$ dB. Given $\mathbf{H}_k$, we define the received SINR of the $k$th user for the SLP scheme with perfect CSI, the non-robust SLP with imperfect CSI and the stochastic robust SLP, respectively, as

$$\mathrm{SINR}_k \triangleq \frac{\mathbb{E}_{\tilde{\mathbf{u}}}\left\{\tilde{\mathbf{u}}^T \mathbf{H}_k^T \mathbf{H}_k \tilde{\mathbf{u}}\right\}}{\sigma_k^2}, \tag{49}$$

$$\mathrm{SINR}_k \triangleq \frac{\mathbb{E}_{\tilde{\mathbf{u}}}\left\{\tilde{\mathbf{u}}^T \mathbf{H}_k^T \mathbf{H}_k \tilde{\mathbf{u}}\right\}}{\sigma_k^2 + \mathbb{E}_{\tilde{\mathbf{u}},\mathbf{E}_k}\left\{\tilde{\mathbf{u}}^T \mathbf{E}_k^T \mathbf{E}_k \tilde{\mathbf{u}}\right\}}, \tag{50}$$

and

$$\begin{aligned}\mathrm{SINR}_k \triangleq (1-\upsilon) \times \frac{\mathbb{E}_{\tilde{\mathbf{u}}}\left\{\tilde{\mathbf{u}}^T \mathbf{H}_k^T \mathbf{H}_k \tilde{\mathbf{u}}\right\}}{\sigma_k^2} \\ + \upsilon \times \frac{\mathbb{E}_{\tilde{\mathbf{u}}}\left\{\tilde{\mathbf{u}}^T \mathbf{H}_k^T \mathbf{H}_k \tilde{\mathbf{u}}\right\}}{\sigma_k^2 + \mathbb{E}_{\tilde{\mathbf{u}},\mathbf{E}_k}\left\{\tilde{\mathbf{u}}^T \mathbf{E}_k^T \mathbf{E}_k \tilde{\mathbf{u}}\right\}}.\end{aligned} \tag{51}$$

where the expectations with respect to $\tilde{\mathbf{u}}$ and $\mathbf{E}_k$ are computed numerically. The SINR quantities in (49), (50) and (51) are then averaged over several realizations of $\mathbf{H}_k$, resulting in the values depicted in Fig. 3 and Fig. 4. We can see from

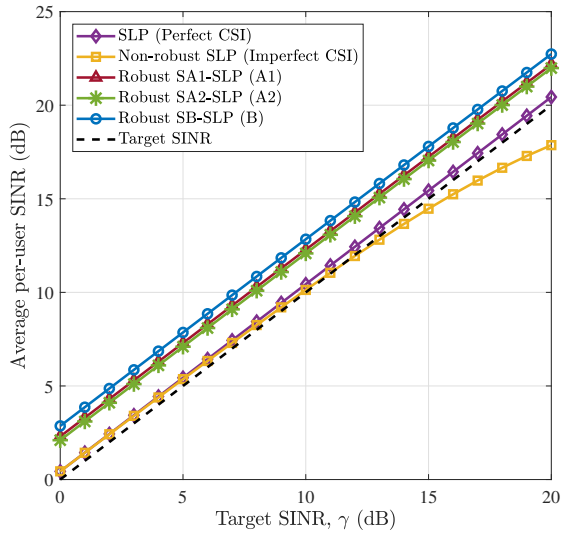


Fig. 3. Average per-user received SINR versus target SINR with $\xi^2 = 0.005$ and $\upsilon = 0.05$.

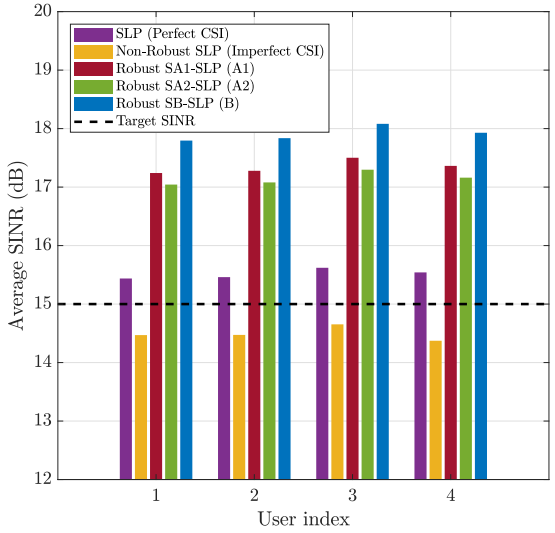


Fig. 4. Average received SINR for different SLP schemes with a target value of $\gamma = 15$ dB, $\xi^2 = 0.005$ and $\upsilon = 0.05$.

Fig. 3 that the given target SINR is likely to not be met by all the users, particularly at high SINR values, when using the non-robust scheme. In fact, the separate bar plot of the received SINR for each user in Fig. 4 shows that at $\gamma = 15$ dB, the SINR requirement has not been satisfied for none of the users by employing the non-robust SLP method. On the other hand, when employing either of the robust approaches, the received SINR of each user is well above the target value. This, however, means that the users are provided with higher SINRs than the required value $\gamma$, which may not be efficient in general. In a practical system design, one needs to reach a compromise based on a specific power-performance tradeoff, according to which the most efficient robust transmission scheme is preferred. We will introduce such a tradeoff and investigate the efficiencies of different approaches later in this section.

In addition to the average received SINR, we are interested in evaluating the probability with which the given target SINR of each user is met. For this purpose, we define "outage event" as a situation in which the minimum required SINR of a user can not be guaranteed. Accordingly, we define the probability of outage for user $k$ as

$$P_{\text{out},k} \triangleq \mathbb{P}\{\text{SINR}_k < \gamma\}. \tag{52}$$

The probability of SINR outage can be equally translated to a rate-outage probability, i.e., the probability that a given target rate $\log_2(1+\gamma)$ is not achievable. This quantity is calculated over many transmissions with different channel realizations and plotted in Fig. 5 as a function of the target SINR $\gamma$ for the non-robust/robust SLP schemes under two different scenarios with $\upsilon = 0.05$, $\xi^2 = 0.005$ and $\upsilon = 0.2$, $\xi^2 = 0.01$. Note that Fig. 5 shows the average probability over all users, i.e., $\bar{P}_{\text{out}} \triangleq (1/K)\sum_{k=1}^{K} P_{\text{out},k}$. As it can be observed, the outage probability increases with $\gamma$ and $\xi^2$. The increasing behavior of $P_{\text{out}}$ with respect to $\gamma$ can be justified from the definitions of $\text{SINR}_k$ in (50) and (51). A larger $\gamma$ results in a

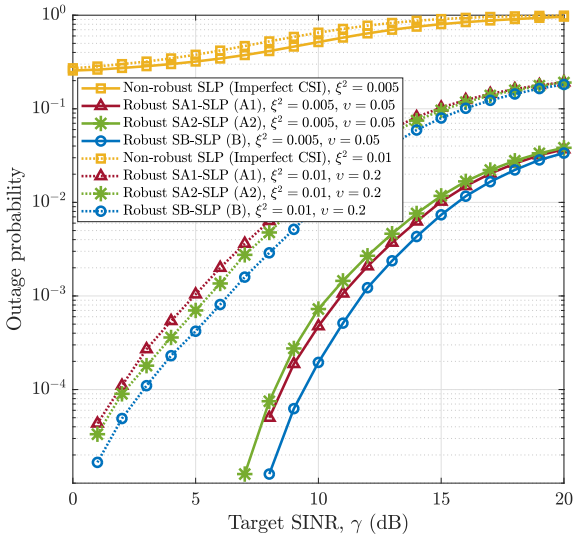


Fig. 5. Probability of outage versus target SINR under two different settings with $\xi^2 = 0.005$, $\upsilon = 0.05$ and $\xi^2 = 0.01$, $\upsilon = 0.2$.

higher transmission power, and subsequently, a greater deal of uncertainty at the receiver side (note that $\mathbf{E}_k\tilde{\mathbf{u}}$ is the uncertain component at the receiver of user $k$). It can be seen that the conservative approach to satisfying the CI constraints taken by the robust methods can lead to significant improvement in the probability of outage compared to the non-robust scheme, i.e., the given target SINR is more probably achievable when employing a robust SLP scheme. Moreover, Fig. 5 shows that each of the SA1-SLP and SA2-SLP methods provides a lower probability of outage compared to the other under different uncertainty settings, while the benchmark SB-SLP approach achieves the lowest outage probability among all in both scenarios.

The higher received SINR and the lower outage probability

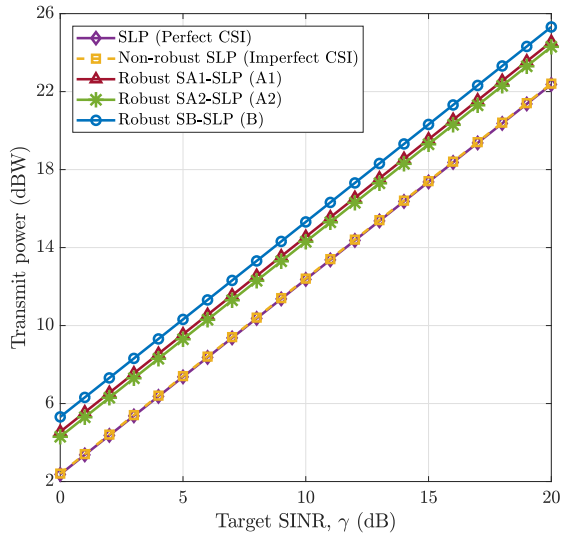


Fig. 6. Average transmission power versus target SINR in a scenario with $\xi^2 = 0.005$ and $\upsilon = 0.05$.

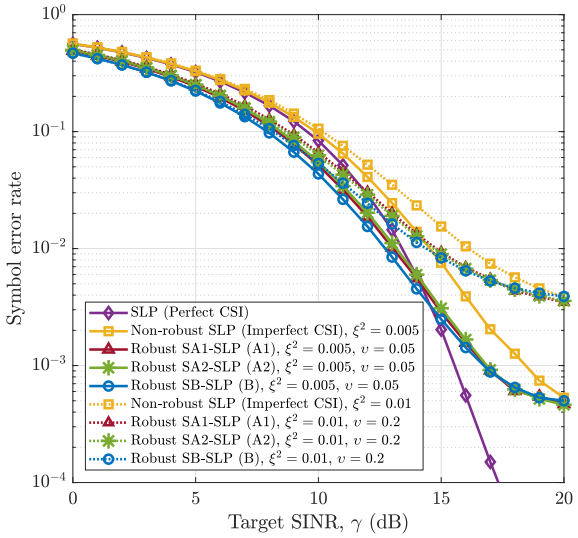


Fig. 8. Average symbol error rate per user versus target SINR for two different scenarios with $\xi^2 = 0.005$, $\upsilon = 0.05$ and $\xi^2 = 0.01$, $\upsilon = 0.2$.

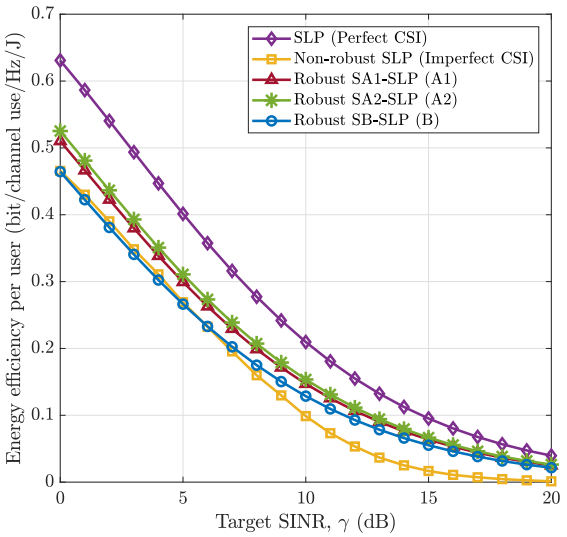


Fig. 7. Energy efficiency comparison of different SLP schemes versus target SINR with $\xi^2 = 0.005$ and $\upsilon = 0.05$.

provided by the robust SLP approaches are, however, results of consuming larger amounts of power for downlink transmission which is inevitable to achieve the desired level of robustness. In Fig. 6, the average total transmit power is depicted versus target SINR, where it is shown that the robust SLP approaches require higher transmission powers than that of the non-robust scheme. A common observation from Fig. 4-6 is that among the robust SLP approaches, the more conservative method with larger transmit power results in higher average received SINR and a lower outage probability for each user.

In order to have a fair and meaningful comparison between the non-robust and robust SLP schemes, we need a measure that incorporates both received SINR and transmit power in evaluating the downlink performance. Inspired by [41], we define "energy efficiency" as the ratio between the expected throughput and the average transmit power. Accordingly, the energy efficiency for the $k$th user, denoted by $\eta_k$, is obtained as

$$\eta_k \triangleq \frac{(1 - P_{\text{out},k})R(\gamma)}{\|\tilde{\mathbf{u}}\|^2}, \tag{53}$$

where $R(\gamma) = \log_2(1+\gamma)$ refers to the achievable transmission rate corresponding to the target SINR $\gamma$. This quantity can be interpreted as the amount of information bits per unit of energy that can be reliably transmitted to each user in one channel use. The average per-user energy efficiency, obtained as $\bar{\eta} \triangleq (1/K)\sum_{k=1}^{K} \eta_k$, is compared for different SLP schemes in Fig. 7. The results show that the proposed robust SLP designs SA1-SLP and SA2-SLP are more energy efficient than the SLP scheme with imperfect CSI as well as the benchmark SB-SLP method. Furthermore, the SA2-SLP design is slightly more energy efficient than SA1-SLP for this particular choice of $\upsilon$, as it is suggested by our tightness analysis in Section IV. We should, however, note that this superiority is obtained in exchange for higher transmitter complexity, as discussed in Section V.

We also plot in Fig. 8 the average per-user symbol error probability obtained by different SLP schemes as a function of SINR requirement $\gamma$. Having imperfect CSI, it can be seen that the non-robust and robust methods both show an error floor at high target SINRs. However, in the whole depicted range of SINR, the robust SLP approaches have lower symbol error rates compared to the non-robust scheme. Furthermore, as it might be expected, increasing $\xi^2$ and $\upsilon$ results in a degraded symbol error rate for the users. In fact, the lower symbol error rate achieved by the robust SLP methods is an advantage of introducing the (robust) CI constraints into the precoder optimization problem.

In order to evaluate the effect of the environment parameter $\xi^2$ on the performance of the symbol-level precoded downlink

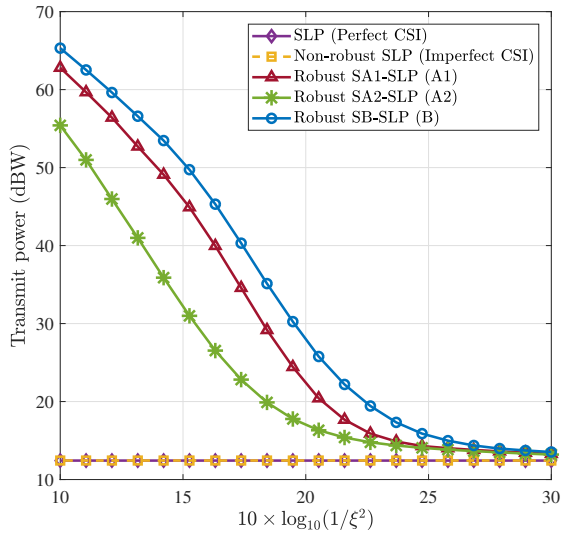


Fig. 9. Average transmission power as a function of uncertainty variance with $\gamma = 10$ dB and $\upsilon = 0.05$.

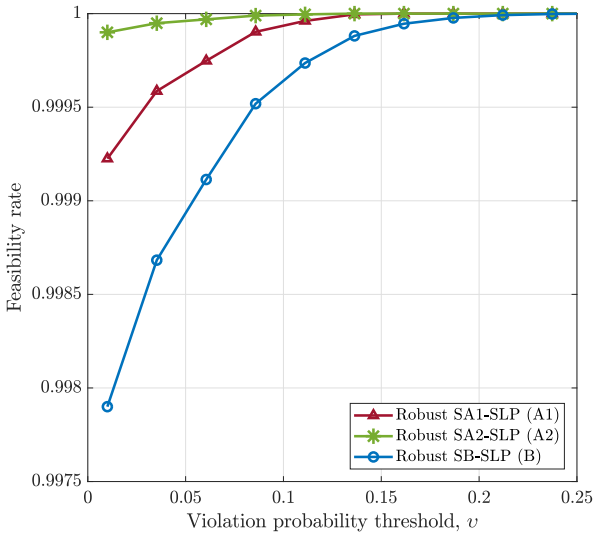


Fig. 11. Feasibility rate as a function of violation probability with $\gamma = 10$ dB and $\xi^2 = 0.01$.

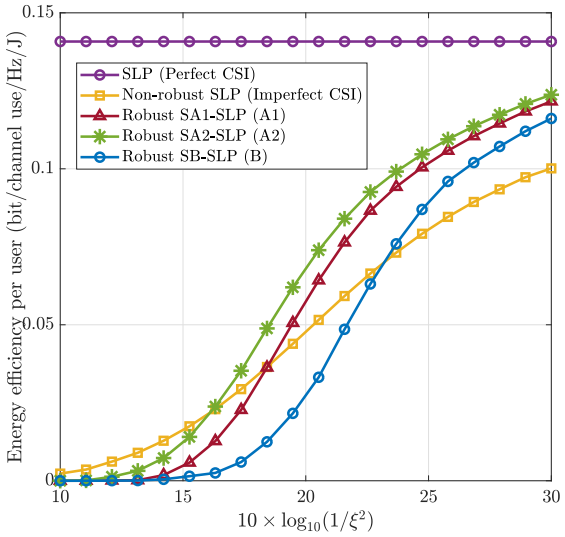


Fig. 10. Per-user energy efficiency as a function of uncertainty variance with $\gamma = 10$ dB and $\upsilon = 0.05$.

transmission, in Fig. 9 and Fig. 10, we respectively plot the average transmit power and the energy efficiency versus $\xi^2$ in an inverse logarithmic scale. From Fig. 9, it can be inferred that for large noise variances, i.e., more severe uncertainty conditions, the robust SLP approaches consume relatively high powers for transmission to ensure a certain level of robustness, while the required transmit power tends to that of the case with perfect CSI as $\xi^2$ decreases. Fig. 10, on the other hand, shows that the energy efficiency under imperfect CSI has an inverse relation to $\xi^2$, i.e., the smaller the noise variance is, the more efficient the SLP scheme will be. This statement is true for both non-robust and robust designs. Although the non-robust scheme shows a superior energy efficiency for large values of $\xi^2$, the SA2-SLP design outperforms the non-robust scheme for $\xi^2 < 0.025$, i.e., $10\log_{10}(1/\xi^2) > 16$ dB in logarithmic scale. Indeed, all the robust approaches are more energy efficient than the non-robust case for relatively small values of the uncertainty variance, i.e., $\xi^2 < 0.005$ corresponding to $10\log_{10}(1/\xi^2) > 23$ dB.

It was previously mentioned in Section V that the robust optimization problem $\mathcal{P}2$ might be infeasible for some values of the violation probability $\upsilon$ and the noise variance $\xi^2$. In particular, having $\upsilon \to 0$ and/or a relatively large value for $\xi^2$ (compared to the spectral norm of the overall channel matrix, i.e., $\|\mathbf{H}\|_2$) increases the probability of $\mathcal{P}2$ being infeasible. In a practical system, a higher rate of feasibility may be reflected in higher service availability to the users. We evaluate this issue through approximating the feasibility rate of the robust SLP approaches over several channel/error/symbol realizations, as shown in Fig. 11 as a function of $\upsilon$. We can see from the figure that both proposed robust SLP designs are feasible, on average, above $\%99$ of the time even for rather small values of $\upsilon$ (i.e., higher levels of conservatism). Apart from the robust design approach, this high feasibility rate is one of the advantages of the symbol-level precoder over conventional block-level techniques, which is mainly due to higher available degrees of freedom in designing the precoder.

Finally, we compare our results with those obtained from the robust block-level precoding scheme proposed in [22], referred to as "robust BLP", which solves a convex semidefinite programming (SDP) to minimize the average transmit power for a given target SINR $\gamma$. It is important to note that the robust BLP approach is barely feasible for large $\gamma$ and $\xi^2$ as well as small values of $\upsilon$ (as we will show in Fig. 15). Therefore, in what follows, we present the results for some limited scenarios with sufficiently small $\gamma$ and $\xi^2$ and large enough $\upsilon$. Furthermore, we average the results obtained form the robust BLP scheme only over those realizations for which the SDP optimization problem in [22] is feasible.

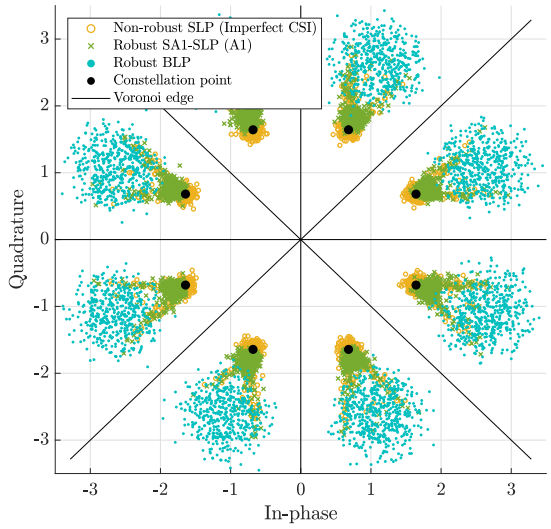


Fig. 12. Scatter plot of the noise-free received signals for 1000 trials with a fixed channel, $\gamma = 5$ dB, $\upsilon = 0.1$ and $\xi^2 = 0.001$.

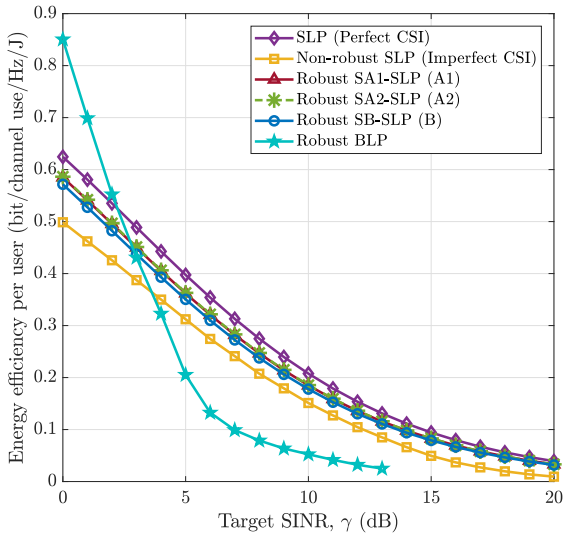


Fig. 13. Energy efficiency comparison of BLP and SLP schemes versus target SINR with $\upsilon = 0.1$ and $\xi^2 = 0.001$.

The scatter plot of the noise-free received signals resulted from the block-level and symbol-level precoding approaches of interest is shown in Fig. 12 for a given target SINR of $\gamma = 5$ dB. In this figure, the average transmit powers of the robust BLP, non-robust SLP and robust SA2-SLP schemes are equal to 8.16 dBW, 8.85 dBW and 11.14 dBW, respectively. The centroids of the received signal clouds corresponding to the robust BLP approach are farther away from the original constellation points which is an expected result of conservative precoding design. This, in turn, increases the consumed transmit power and accordingly reduces the energy efficiency for high target SINR values, as we will see later.

In Fig. 13, we compare the energy efficiency of different non-robust/robust precoding schemes as a function of the target SINR $\gamma$. Using the robust BLP method, for given $\mathbf{h}_k$, the received SINR of the $k$th user is given by

$$\mathrm{SINR}_k \triangleq \frac{\mathbf{t}_k^H \mathbf{h}_k^H \mathbf{h}_k \mathbf{t}_k}{\sigma_k^2 + \sum_{j \neq k} \mathbf{t}_j^H \mathbf{h}_k^H \mathbf{h}_k \mathbf{t}_j}, \tag{54}$$

where $\mathbf{t}_k$ is the precoding vector that corresponds to user $k$. It can be seen from Fig. 13 that the robust BLP scheme is more energy efficient than all the robust SLP approaches at low target SINRs up to $\sim 3$ dB. Recall that the results are averaged only over those realizations for which the robust BLP is feasible, i.e., we do not take the infeasibility rate into account in our performance comparisons. On the contrary, for moderate-to-high SINR values, the proposed SLP approaches outperform the robust BLP scheme. Notice also that the optimization problem of the robust BLP scheme was infeasible in all our trials with $\gamma \geq 14$ dB. This in mainly due to the fact that the robust BLP scheme requires an infinite transmit power (i.e., the optimization problem is practically infeasible) from a certain target SINR value on. However, the feasibility of the proposed robust SLP approaches does not depend on $\gamma$. Furthermore, the energy efficiency of the precoding schemes of interest as a function of the violation probability is plotted

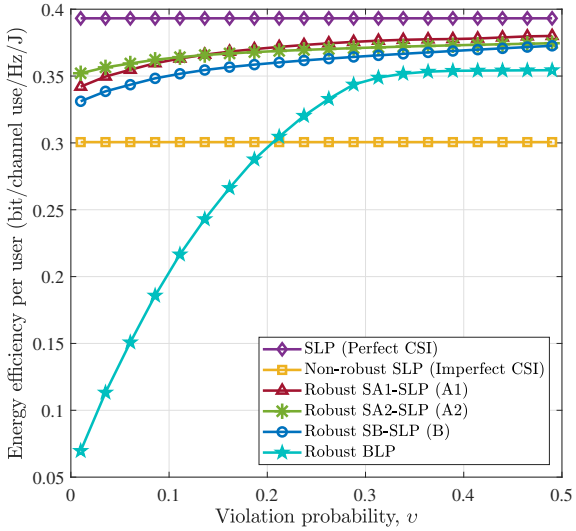


Fig. 14. Per-user energy efficiency as a function of violation probability with $\gamma = 5$ dB and $\xi^2 = 0.001$.

in Fig. 14, where it is shown that the proposed robust SLP approaches outperform the robust BLP method for all values of $\upsilon \in (0, 1/2]$ in the considered setting. It further follows from Fig. 14 that the energy efficiency of the proposed robust SLP approaches tend to that of the SLP scheme with perfect CSI as $\upsilon$ increases.

The feasibility rates of the robust block-level and symbol-level precoders are compared in Fig. 15 as a function of the uncertainty variance $\xi^2$ in an inverse logarithmic scale. As it can be seen, both SA1-SLP and SA2-SLP methods are feasible more than %93 of the time in the whole evaluated range of $\xi^2$. In particular, both our proposed robust approaches are %100 feasible for $\xi^2 < 0.015$, or $10 \log_{10}(1/\xi^2) > 18$ dB. The robust BLP scheme, on the other hand, is %50 or higher feasible only

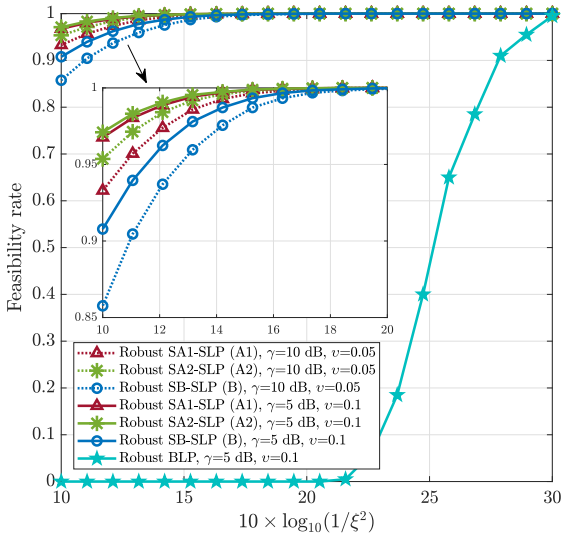


Fig. 15. Feasibility rate comparison of different robust precoding approaches as a function of uncertainty variance with $\gamma = 5$ dB, $\upsilon = 0.1$ and $\gamma = 10$ dB, $\upsilon = 0.05$.

for $\xi^2 < 0.003$, i.e, $10\log_{10}(1/\xi^2) > 25$ dB, while it appears to be barely feasible for uncertainty variances larger than $0.01$.

It should be noted that the improved feasibility rate and energy efficiency of an SLP scheme compared to a block-level approach is obtained at the cost of per-symbol optimization of the precoded signal, which may lead to higher transmitter complexity. To have an illustrative comparison of complexity, consider the robust BLP method in [22]. This method needs to solve an optimization problem with SDP and SOC constraints of dimension $2(2N+1)(K+1)$ and $4NK+1$, respectively. Roughly speaking, the worst-case complexity of finding an $\epsilon$-optimal solution via a standard interior-point method is of order $\mathcal{O}(K^6N^6)\ln(1/\epsilon)$, where such a solution has to be obtained once the CSI is updated. On the other hand, the arithmetic complexity of the proposed robust SLP approaches have been shown to be $\mathcal{O}(K\sqrt{K}N^3)\ln(1/\epsilon)$; see Table II. We recall that the symbol-level precoded transmit signal needs to be redesigned as many times as either the frame length or the total number of possible symbol realizations for $K$ users, i.e., $M^K$ where $M$ is the modulation order. Denoting by $S$ the number of information symbols per a single transmitted frame, the overall (per CSI update) complexity of an SLP scheme can be approximated as $\min\{S, M^K\}.\mathcal{O}(K\sqrt{K}N^3)\ln(1/\epsilon)$. Hence, a relative computation cost between the robust SLP and BLP methods, in the limiting case, is given by the ratio $\min\{S, M^K\}/K^4\sqrt{K}N^3$. In particular, for moderate number of users and low-order modulation schemes, the computational cost of a symbol-level precoder can be alleviated by an offline optimization of the precoded signals and using a lookup table for downlink transmission [8]. Moreover, it might be possible to derive low-complexity (semi closed-form) solutions for the robust SLP approaches, similar to those obtained in [42]–[44] for the original SINR-constrained SLP power minimization problem, which can be the topic of a future work.

## VII. Conclusions and Future Work

We addressed the robust design problem of symbol-level precoded transmission scheme in a downlink MU-MISO system under imperfect stochastic CSI knowledge at the transmitter. We considered a QoS-constrained design criterion aimed at minimizing the total instantaneous (per-symbol) transmit power subject to constructive interference (CI) constraints as well as given target SINRs. A probabilistic approach was then adopted to imply the optimization constraints, which led us to intractable expressions. We tackled this difficulty by deriving two computationally tractable approximate convex constraints with different levels of conservatism. A benchmark approximation was also derived based on the sphere bounding conservative method. Our analytical and simulation results showed that both the proposed robust convex approximations outperform the benchmark, while each of them is superior to the other under different robustness settings. In comparison with a conventional block-level robust scheme, the proposed robust methods was shown to be more efficient at moderate-to-high target SINR values. However, a more considerable advantage of the proposed robust SLP approaches is their higher feasibility rate for wide ranges of violation probability and uncertainty variance, which is indifferent to the target SINR. We also highlight from our complexity analysis that the improved performances of the proposed robust SLP designs come with an increased computational complexity by an order of the number of users in the limiting case.

It would be an interesting problem to extend the current results to a more general case, i.e., having inner points in the constellation for which the distance preserving CI regions are only the constellation points. In such a case, the CI chance constraint corresponding to an inner constellation point will always have an empty feasible region, so does the robust SLP optimization problem. In order to generalize the current approach to the case with multi-level modulation schemes, one may define a relaxed CI region around an inner constellation point, allowing the noise-free received signal to lie within the relaxed region. This relaxation may affect the symbol error rate performance at the receiver side, but on the other hand may result in a lower transmission power. Therefore, one also needs to carefully choose the amount of relaxation such that a certain performance level is guaranteed. In general, this might be rather challenging and the design approach may need to be done analytically by taking the given system/user requirements into account, which is beyond the scope of this paper and can be considered as a future work.

## Appendix A
## Proof of equality (b) in (15)

First, let $\mathbf{Q}_k \triangleq \mathbb{E}\{\mathrm{vec}(\mathbf{E}_k)\mathrm{vec}(\mathbf{E}_k)^T\}$ denote the covariance matrix of $\mathrm{vec}(\mathbf{E}_k)$ as given in (13). It follows that

$$\mathbf{Q}_k = \frac{1}{2}\,\xi_k^2 \begin{bmatrix} \mathbf{I}_N \otimes \mathbf{I}_2 & \mathbf{I}_N \otimes \mathbf{J}_2 \\ \mathbf{I}_N \otimes \mathbf{J}_2^T & \mathbf{I}_N \otimes \mathbf{I}_2 \end{bmatrix}, \tag{55}$$

where we have used the facts that $(\mathbf{I}_N \otimes \mathbf{J}_2)^T = \mathbf{I}_N \otimes \mathbf{J}_2^T$ and $\mathbf{I}_{2N} = \mathbf{I}_N \otimes \mathbf{I}_2$. Now, the desired equality to be proven can be written as

$$(\tilde{\mathbf{u}}^T \otimes \mathbf{A}_k)\, \mathbf{Q}_k (\tilde{\mathbf{u}} \otimes \mathbf{A}_k^T) = \frac{1}{2}\, \xi_k^2\, (\tilde{\mathbf{u}}^T \otimes \mathbf{A}_k)(\tilde{\mathbf{u}} \otimes \mathbf{A}_k^T), \tag{56}$$

Using the property $(\tilde{\mathbf{u}}^T \otimes \mathbf{A}_k)(\tilde{\mathbf{u}} \otimes \mathbf{A}_k^T) = (\tilde{\mathbf{u}}^T \tilde{\mathbf{u}}) \otimes (\mathbf{A}_k \mathbf{A}_k^T)$, equivalently, it is desired that

$$(\tilde{\mathbf{u}}^T \otimes \mathbf{A}_k)\, \mathbf{Q}_k (\tilde{\mathbf{u}} \otimes \mathbf{A}_k^T) = \frac{1}{2}\, \xi_k^2\, \|\tilde{\mathbf{u}}\|^2 (\mathbf{A}_k \mathbf{A}_k^T), \tag{57}$$

We proceed by focusing on the left-hand side of (57). Let us denote $(\tilde{\mathbf{u}}^T \otimes \mathbf{A}_k)\mathbf{Q}_k(\tilde{\mathbf{u}} \otimes \mathbf{A}_k^T) \triangleq \mathbf{G} = [g_{ij}]_{2\times 2}$ and $\tilde{\mathbf{u}}^T = [\mathbf{u}_{\mathrm{R}}^T, \mathbf{u}_{\mathrm{I}}^T]$, where $\mathbf{u}_{\mathrm{R}} = \mathrm{Re}(\mathbf{u})$ and $\mathbf{u}_{\mathrm{I}} = \mathrm{Im}(\mathbf{u})$. Thus, considering $\mathbf{A}_k = [\mathbf{a}_{k,1}, \mathbf{a}_{k,2}]^T$, we have

$$\begin{aligned}\mathbf{G} = \frac{1}{2}\, \xi_k^2 & \begin{bmatrix} \mathbf{u}_{\mathrm{R}}^T \otimes \mathbf{a}_{k,1}^T & \mathbf{u}_{\mathrm{I}} \otimes \mathbf{a}_{k,1}^T \\ \mathbf{u}_{\mathrm{R}}^T \otimes \mathbf{a}_{k,2}^T & \mathbf{u}_{\mathrm{I}} \otimes \mathbf{a}_{k,2}^T \end{bmatrix} \\ & \times \begin{bmatrix} \mathbf{I}_N \otimes \mathbf{I}_2 & \mathbf{I}_N \otimes \mathbf{J}_2 \\ \mathbf{I}_N \otimes \mathbf{J}_2^T & \mathbf{I}_N \otimes \mathbf{I}_2 \end{bmatrix} \times \begin{bmatrix} \mathbf{u}_{\mathrm{R}} \otimes \mathbf{a}_{k,1} & \mathbf{u}_{\mathrm{R}} \otimes \mathbf{a}_{k,2} \\ \mathbf{u}_{\mathrm{I}} \otimes \mathbf{a}_{k,1} & \mathbf{u}_{\mathrm{I}} \otimes \mathbf{a}_{k,2} \end{bmatrix}. \end{aligned} \tag{58}$$

Foe the sake of simplicity, the term $\frac{1}{2}\,\xi_k^2$ is omitted from the next equation, but it will appear in the final derivation. The matrix multiplication in the right-hand side of (58) can be evaluated and simplified as

$$g_{11} = \left(\mathbf{u}_{\mathrm{R}}^T \mathbf{u}_{\mathrm{R}} + \mathbf{u}_{\mathrm{I}}^T \mathbf{u}_{\mathrm{I}}\right) \mathbf{a}_{k,1}^T \mathbf{a}_{k,1} + 2\, \mathbf{u}_{\mathrm{R}}^T \mathbf{u}_{\mathrm{I}} \otimes \mathbf{a}_{k,1}^T \mathbf{J}_2 \mathbf{a}_{k,1}, \tag{59a}$$

$$\begin{aligned} g_{12} = g_{21} = & \left(\mathbf{u}_{\mathrm{R}}^T \mathbf{u}_{\mathrm{R}} + \mathbf{u}_{\mathrm{I}}^T \mathbf{u}_{\mathrm{I}}\right) \mathbf{a}_{k,1}^T \mathbf{a}_{k,2} \\ & + 2\, \mathbf{u}_{\mathrm{R}}^T \mathbf{u}_{\mathrm{I}} \otimes \left(\mathbf{a}_{k,1}^T \mathbf{J}_2 \mathbf{a}_{k,2} + \mathbf{a}_{k,1}^T \mathbf{J}_2^T \mathbf{a}_{k,2}\right). \end{aligned} \tag{59b}$$

$$g_{22} = \left(\mathbf{u}_{\mathrm{R}}^T \mathbf{u}_{\mathrm{R}} + \mathbf{u}_{\mathrm{I}}^T \mathbf{u}_{\mathrm{I}}\right) \mathbf{a}_{k,2}^T \mathbf{a}_{k,2} + 2\, \mathbf{u}_{\mathrm{R}}^T \mathbf{u}_{\mathrm{I}} \otimes \mathbf{a}_{k,2}^T \mathbf{J}_2 \mathbf{a}_{k,2}, \tag{59c}$$

where in simplifications, we have frequently used the fact that $(\mathbf{X} \otimes \mathbf{Y})(\mathbf{W} \otimes \mathbf{Z}) = (\mathbf{XW} \otimes \mathbf{YZ})$, for any given matrices $\mathbf{X}, \mathbf{Y}, \mathbf{W}, \mathbf{Z}$ with appropriate dimensions. It is easy to verify that $\mathbf{a}_{k,1}^T \mathbf{J}_2 \mathbf{a}_{k,1} = \mathbf{a}_{k,1}^T \mathbf{J}_2^T \mathbf{a}_{k,1} = \mathbf{0}$, and further $\mathbf{a}_{k,1}^T \mathbf{J}_2 \mathbf{a}_{k,2} + \mathbf{a}_{k,1}^T \mathbf{J}_2^T \mathbf{a}_{k,2} = \mathbf{a}_{k,1}^T (\mathbf{J}_2 + \mathbf{J}_2^T) \mathbf{a}_{k,2} = \mathbf{0}$. Moreover, it directly follows from the definition of $\tilde{\mathbf{u}}$ that $\mathbf{u}_{\mathrm{R}}^T \mathbf{u}_{\mathrm{R}} + \mathbf{u}_{\mathrm{I}}^T \mathbf{u}_{\mathrm{I}} = \tilde{\mathbf{u}}^T \tilde{\mathbf{u}}$. Applying all these notes to (59a)-(59c), the entries of $\mathbf{G}$ are obtained as

$$g_{11} = \|\tilde{\mathbf{u}}\|^2 \|\mathbf{a}_{k,1}\|^2, \tag{60a}$$

$$g_{12} = g_{21} = \|\tilde{\mathbf{u}}\|^2\, \mathbf{a}_{k,1}^T \mathbf{a}_{k,2}, \tag{60b}$$

$$g_{22} = \|\tilde{\mathbf{u}}\|^2 \|\mathbf{a}_{k,2}\|^2. \tag{60c}$$

Merging the results in (60) yields

$$\mathbf{G} = \frac{1}{2}\, \xi_k^2\, \|\tilde{\mathbf{u}}\|^2 (\mathbf{A}_k \mathbf{A}_k^T), \tag{61}$$

as required.

## Appendix B
## Derivation of equivalent SOC formulation for A2

The derivation is essentially based on Lemma 1. We denote

$$\mathbf{X} \triangleq \begin{bmatrix} -\frac{\bar{w}_{k,1}}{\psi(\upsilon)} & 0 \\ 0 & -\frac{\bar{w}_{k,2}}{\psi(\upsilon)} \end{bmatrix}, \quad \mathbf{Y} \triangleq \begin{bmatrix} 1 & 0 & 0 & 0 \\ 0 & 0 & 0 & 1 \end{bmatrix},$$

$$\mathbf{Z} \triangleq \begin{bmatrix} -\frac{\bar{w}_{k,1}}{\psi(\upsilon)} & 0 & 0 & 0 \\ 0 & -\frac{\bar{w}_{k,2}}{\psi(\upsilon)} & 0 & 0 \\ 0 & 0 & -\frac{\bar{w}_{k,1}}{\psi(\upsilon)} & 0 \\ 0 & 0 & 0 & -\frac{\bar{w}_{k,2}}{\psi(\upsilon)} \end{bmatrix}.$$

Accordingly, the constraint (32) can be equivalently implied by the following two semidefinite restrictions:

$$\mathbf{X} \succeq 0, \tag{62a}$$

$$\mathbf{Z} - \mathbf{Y}^T \mathbf{X}^{-1} \mathbf{Y} \succeq 0. \tag{62b}$$

The second restriction in (62b), after doing the matrix products and some simple algebra, can be written as

$$\begin{bmatrix} -\frac{\bar{w}_{k,1}}{\psi(\upsilon)} + \frac{\psi(\upsilon)}{\bar{w}_{k,1}} & 0 & 0 & 0 \\ 0 & -\frac{\bar{w}_{k,1}}{\psi(\upsilon)} & 0 & 0 \\ 0 & 0 & -\frac{\bar{w}_{k,2}}{\psi(\upsilon)} & 0 \\ 0 & 0 & 0 & -\frac{\bar{w}_{k,2}}{\psi(\upsilon)} + \frac{\psi(\upsilon)}{\bar{w}_{k,2}} \end{bmatrix} \succeq 0. \tag{63}$$

from which it is clear that (62b) further implies the restriction $\mathbf{X} \succeq 0$, hence it is necessary and sufficient for (32). We then rearrange (63) in a more convenient form and decompose it into two semidefinite constraints as

$$\frac{-1}{\psi(\upsilon)}\, \mathbf{D}_{\bar{\mathbf{w}}_k} \succeq 0, \tag{64a}$$

$$\frac{-1}{\psi(\upsilon)}\, \mathbf{D}_{\bar{\mathbf{w}}_k} + \psi(\upsilon)\, \mathbf{D}_{\bar{\mathbf{w}}_k}^{-1} \succeq 0, \tag{64b}$$

with $\mathbf{D}_{\bar{\mathbf{w}}_k} \triangleq \mathrm{diag}(\bar{\mathbf{w}}_k)$. It should be noticed that the restriction (64a) is in fact equivalent to $\mathbf{D}_{\bar{\mathbf{w}}_k} \preceq 0$ or $\bar{\mathbf{w}}_k \leq \mathbf{0}$, which is implied by the constraint $\mathbf{w}_k \leq \mathbf{0}$; see Remark 1. Further, note that $\mathrm{erfc}(\cdot)$ is non-negative in the interval $(0, 1]$, so is $\psi(\upsilon)$. Now, multiplying both sides of (64b) by $\mathbf{D}_{\bar{\mathbf{w}}_k}$, and imposing the restriction (64a) which changes the direction of the inequality, both of the constraints (64b) and (64a) can be simultaneously expressed by

$$\frac{-1}{\psi(\upsilon)}\, \mathbf{D}_{\bar{\mathbf{w}}_k}^2 + \psi(\upsilon)\, \mathbf{I} \preceq 0. \tag{65}$$

Since $\mathbf{D}_{\bar{\mathbf{w}}_k} \preceq 0$ and diagonal, from (65) by taking square root, we obtain

$$\frac{1}{\psi(\upsilon)}\, \mathbf{D}_{\bar{\mathbf{w}}_k} + \mathbf{I} \preceq 0, \tag{66}$$

which can be written in the vector form as

$$\frac{-1}{\psi(\upsilon)}\, \bar{\mathbf{w}}_k \geq \mathbf{1}. \tag{67}$$

Replacing $\bar{\mathbf{w}}_k$ with $(\sqrt{2}/\xi_k \|\tilde{\mathbf{u}}\|)(\mathbf{A}_k \mathbf{A}_k^T)^{-1/2} \mathbf{w}_k(\tilde{\mathbf{u}})$, it is then routine to show that (67) is equivalent to

$$\|\tilde{\mathbf{u}}\|\, \mathbf{1} \leq \frac{-\sqrt{2}}{\psi(\upsilon)\, \xi_k} (\mathbf{A}_k \mathbf{A}_k^T)^{-1/2} \mathbf{w}_k(\tilde{\mathbf{u}}), \tag{68}$$


## Acknowledgment

The authors are supported by the Luxembourg National Research Fund (FNR) under CORE Junior project: C16/IS/11332341 Enhanced Signal Space opTImization for satellite comMunication Systems (ESSTIMS).

## REFERENCES


[1] A. B. Gershman, N. D. Sidiropoulos, S. Shahbazpanahi, M. Bengtsson, and B. Ottersten, "Convex optimization-based beamforming," *IEEE Signal Process. Mag.*, vol. 27, no. 3, pp. 62–75, May 2010.

[2] E. Visotsky and U. Madhow, "Optimum beamforming using transmit antenna arrays," in *1999 IEEE 49th Vehicular Technology Conference (Cat. No.99CH36363)*, vol. 1, Jul. 1999, pp. 851–856 vol.1.

[3] M. Schubert and H. Boche, "Solution of the multiuser downlink beamforming problem with individual SINR constraints," *IEEE Trans. Veh. Technol.*, vol. 53, no. 1, pp. 18–28, Jan. 2004.

[4] E. Björnson, M. Bengtsson, and B. Ottersten, "Optimal multiuser transmit beamforming: A difficult problem with a simple solution structure," *IEEE Signal Process. Mag.*, vol. 31, no. 4, pp. 142–148, Jul. 2014.

[5] M. Bengtsson and B. Ottersten, *Handbook of Antennas in Wireless Communications*, 2001, ch. Optimal and suboptimal transmit beamforming.

[6] C. B. Peel, B. M. Hochwald, and A. L. Swindlehurst, "A vector-perturbation technique for near-capacity multiantenna multiuser communication-part I: channel inversion and regularization," *IEEE Trans. Commun.*, vol. 53, no. 1, pp. 195–202, Jan. 2005.

[7] C. Masouros, T. Ratnarajah, M. Sellathurai, C. B. Papadias, and A. K. Shukla, "Known interference in the cellular downlink: a performance limiting factor or a source of green signal power?" *IEEE Commun. Mag.*, vol. 51, no. 10, pp. 162–171, Oct. 2013.

[8] M. Alodeh, S. Chatzinotas, and B. Ottersten, "Constructive multiuser interference in symbol level precoding for the MISO downlink channel," *IEEE Trans. Signal Process.*, vol. 63, no. 9, pp. 2239–2252, May 2015.

[9] D. J. Love, R. W. Heath, W. Santipach, and M. L. Honig, "What is the value of limited feedback for mimo channels?" *IEEE Commun. Mag.*, vol. 42, no. 10, pp. 54–59, Oct. 2004.

[10] N. Jindal, "MIMO broadcast channels with finite-rate feedback," *IEEE Trans. Inform. Theory*, vol. 52, no. 11, pp. 5045–5060, Nov. 2006.

[11] T. Weber, A. Sklavos, and M. Meurer, "Imperfect channel-state information in MIMO transmission," *IEEE Trans. Commun.*, vol. 54, no. 3, pp. 543–552, Mar. 2006.

[12] M. Payaro, A. Pascual-Iserte, and M. A. Lagunas, "Robust power allocation designs for multiuser and multiantenna downlink communication systems through convex optimization," *IEEE J. Sel. Areas in Commun.*, vol. 25, no. 7, pp. 1390–1401, Sep. 2007.

[13] A. Pascual-Iserte, D. P. Palomar, A. I. Perez-Neira, and M. A. Lagunas, "A robust maximin approach for MIMO communications with imperfect channel state information based on convex optimization," *IEEE Trans. Signal Process.*, vol. 54, no. 1, pp. 346–360, Jan. 2006.

[14] H. V. Poor, *An introduction to signal detection and estimation*. Springer Science & Business Media, 2013.

[15] I. Wajid, M. Pesavento, Y. C. Eldar, and D. Ciochina, "Robust downlink beamforming with partial channel state information for conventional and cognitive radio networks," *IEEE Trans. Signal Process.*, vol. 61, no. 14, pp. 3656–3670, Jul. 2013.

[16] M. B. Shenouda and T. N. Davidson, "Convex conic formulations of robust downlink precoder designs with quality of service constraints," *IEEE J. Sel. Topics Signal Process.*, vol. 1, no. 4, pp. 714–724, Dec. 2007.

[17] A. Abdel-Samad, T. N. Davidson, and A. B. Gershman, "Robust transmit eigen beamforming based on imperfect channel state information," *IEEE Trans. Signal Process.*, vol. 54, no. 5, pp. 1596–1609, May 2006.

[18] M. B. Shenouda and T. N. Davidson, "Nonlinear and linear broadcasting with QoS requirements: Tractable approaches for bounded channel uncertainties," *IEEE Trans. Signal Process.*, vol. 57, no. 5, pp. 1936–1947, May. 2009.

[19] N. Vucic and H. Boche, "Robust QoS-constrained optimization of downlink multiuser MISO systems," *IEEE Trans. Signal Process.*, vol. 57, no. 2, pp. 714–725, Feb. 2009.

[20] X. Zhang, D. P. Palomar, and B. Ottersten, "Statistically robust design of linear MIMO transceivers," *IEEE Trans. Signal Process.*, vol. 56, no. 8, pp. 3678–3689, Aug. 2008.

[21] N. Vucic and H. Boche, "A tractable method for chance-constrained power control in downlink multiuser MISO systems with channel uncertainty," *IEEE Signal Process. Lett.*, vol. 16, no. 5, pp. 346–349, May 2009.

[22] M. Botros Shenouda and T. N. Davidson, "Probabilistically-constrained approaches to the design of the multiple antenna downlink," in *2008 42nd Asilomar Conf. Signals, Systems and Computers*, Oct. 2008, pp. 1120–1124.

[23] B. K. Chalise, S. Shahbazpanahi, A. Czylwik, and A. B. Gershman, "Robust downlink beamforming based on outage probability specifications," *IEEE Trans. Wirel. Commun.*, vol. 6, no. 10, pp. 3498–3503, Oct. 2007.

[24] B. K. Chalise and A. Czylwik, "Robust uplink beamforming based upon minimum outage probability criterion," in *Global Telecommun. Conf., 2004. GLOBECOM '04. IEEE*, vol. 6, Nov. 2004, pp. 3974–3978 Vol.6.

[25] K. Wang, A. M. So, T. Chang, W. Ma, and C. Chi, "Outage constrained robust transmit optimization for multiuser MISO downlinks: Tractable approximations by conic optimization," *IEEE Transactions on Signal Processing*, vol. 62, no. 21, pp. 5690–5705, Nov. 2014.

[26] A. Ben-Taly and A. Nemirovskiz, "On safe tractable approximations of chance constrained linear matrix inequalities," *Mathematics of Operations Research*, vol. 34, no. 1, pp. 1–25, Feb. 2009.

[27] D. Bertsimas and M. Sim, "Tractable approximations to robust conic optimization problems," *Mathematics of Operations Research*, vol. 107, no. 1-2, pp. 5–36, Jun. 2006.

[28] C. Masouros and G. Zheng, "Exploiting known interference as green signal power for downlink beamforming optimization," *IEEE Trans. Signal Process.*, vol. 63, no. 14, pp. 3628–3640, Jul. 2015.

[29] M. R. A. Khandaker, C. Masouros, K. Wong, and S. Timotheou, "Secure SWIPT by exploiting constructive interference and artificial noise," *IEEE Trans. Commun.*, vol. 67, no. 2, pp. 1326–1340, Feb. 2019.

[30] K. L. Law and C. Masouros, "Constructive interference exploitation for downlink beamforming based on noise robustness and outage probability," in *2016 IEEE Int. Conf. Acoustics, Speech and Signal Process. (ICASSP)*, Mar. 2016, pp. 3291–3295.

[31] A. Haqiqatnejad, F. Kayhan, and B. Ottersten, "Constructive interference for generic constellations," *IEEE Signal Process. Lett.*, vol. 25, no. 4, pp. 586–590, Apr. 2018.

[32] D. P. Palomar, "A unified framework for communications through MIMO channels," Ph.D. dissertation, Technical University of Catalonia (UPC), 2003.

[33] T. Yoo and A. Goldsmith, "Capacity and power allocation for fading MIMO channels with channel estimation error," *IEEE Transactions on Information Theory*, vol. 52, no. 5, pp. 2203–2214, May 2006.

[34] A. Haqiqatnejad, F. Kayhan, and B. Ottersten, "Symbol-level precoding design based on distance preserving constructive interference regions," *IEEE Trans. Signal Process.*, vol. 66, no. 22, pp. 5817–5832, Nov. 2018.

[35] ——, "Power minimizer symbol-level precoding: A closed-form suboptimal solution," *IEEE Signal Processing Letters*, vol. 25, no. 11, pp. 1730–1734, Nov. 2018.

[36] D. Tse and P. Viswanath, *Fundamentals of wireless communication*. Cambridge university press, 2005.

[37] A. L. Agnan Kessy and K. Strimmer, "Optimal whitening and decorrelation," *The American statistician*, pp. 1–6, Dec. 2016.

[38] S. Boyd and L. Vandenberghe, *Convex Optimization*. Cambridge Univ. Press, 2004.

[39] A. Ben-Tal and A. Nemirovski, *Lectures on modern convex optimization*. Siam, 2001, vol. 2.

[40] J. F. Sturm, "Using SeDuMi 1.02, a Matlab toolbox for optimization over symmetric cones," *Optimization Methods and Software*, vol. 11, no. 1-4, pp. 625–653, 1999.

[41] E. V. Belmega and S. Lasaulce, "Energy-efficient precoding for multiple-antenna terminals," *IEEE Trans. Signal Process.*, vol. 59, no. 1, pp. 329–340, Jan. 2011.

[42] A. Li and C. Masouros, "Interference exploitation precoding made practical: Optimal closed-form solutions for PSK modulations," *IEEE Trans. Wirel. Commun.*, vol. 17, no. 11, pp. 7661–7676, 2018.

[43] A. Haqiqatnejad, F. Kayhan, and B. Ottersten, "An approximate solution for symbol-level multiuser precoding using support recovery," in *2019 IEEE 20th Int. Workshop Signal Process. Advances in Wirel. Commun. (SPAWC)*, Jul. 2019, pp. 1–5.

[44] S. A. S. C. Jevgenij Krivochiza, J.C. Merlano-Duncan and B. Ottersten, "Closed-form solution for computationally efficient symbol-level precoding," in *2018 IEEE Global Communications Conference (GLOBECOM)*, Sep. 2018.